AcouST

Acoustic Simulation TOol

Book of Tutorials

v2.0

Umberto Iemma & Vincenzo Marchese
http://acousto.sourceforge.net

Contents

1 Scattering of spherical waves by a rigid sphere **4**

1.1 Analytical solution 5

1.2 Files 6

1.3 Setting up 6

1.3.1 Using the built–in `AcouSTO` pre–processor 6

1.3.2 Using `Gmsh` 7

1.4 Analysis of results 9

1.4.1 Influence of the reduced frequency, ka 10

1.4.2 Symmetry management 11

1.4.3 Primary field formulation 11

1.4.4 Regularization at spurious eigenfrequencies 12

2 Scattering of a plane wave by an impedance sphere **13**

2.1 Analytical solution 14

2.2 Files 14

2.3 `AcouSTO` solution using the *impedance body* option 14

2.4 `AcouSTO` solution using an impedance file 15

2.5 AcouSTO solution using custom boundary conditions 17

3 Engines' shielding effect of an aircraft model in static conditions 20

3.1 Description 21

3.2 Files 21

3.3 How to use it 22

3.4 Results 23

4 Frequency response of a $E_\flat$–tuned natural trumpet 26

4.1 Files 27

4.2 How to use it 27

4.3 Results 28

4.3.1 Input impedance of the instrument 28

5 A simple radiating box 30

5.1 Files 31

5.2 Geometry generation and simulation 31

6 Just a bit of room acoustics 35

6.1 Files 36

6.2 Response with sound–hard walls 37

6.3 Analysis with one sound–absorbing wall 38

6.3.1 Source strength definition 38

6.3.2 Wall impedance 40

6.3.3 Application 41

© U. Iemma & V. Marchese

7 Incompressible Potential Aerodynamics **43**

7.1 Potential flow of an incompressible, inviscid fluid 44

7.2 Files 45

7.3 Impermeable sphere in a uniform flow 45

7.3.1 How to solve the problem with `AcouSTO` 45

© U. Iemma & V. Marchese

CHAPTER 1

Scattering of spherical waves by a rigid sphere

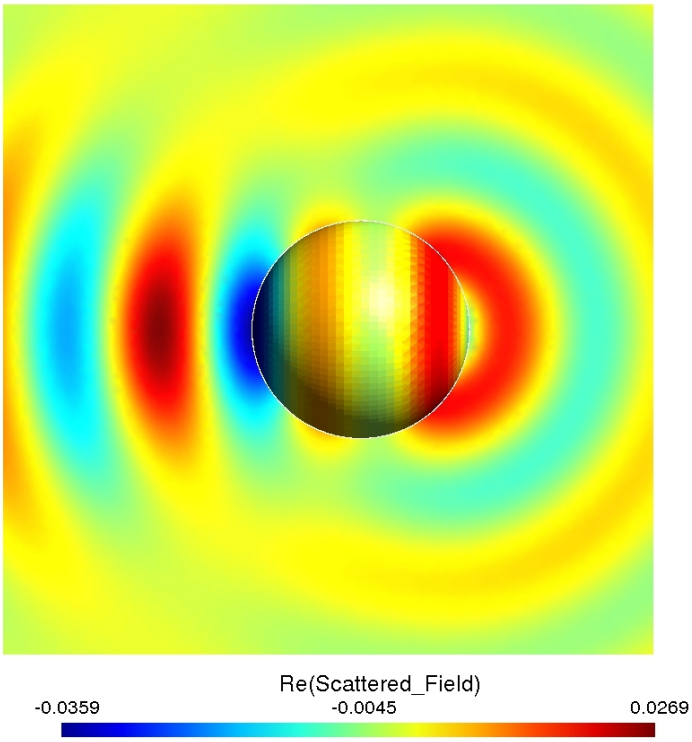

A simple problem to learn about symmetries

Aim of this first tutorial is to familiarize with the basic features of `AcouSTO` with the very simple problem of the scattering of the field induced by a monopole due to a sound–hard sphere of radius $a = 1$. An axially symmetric configuration is chosen to let the user verify by himself the different options available to handle symmetries. In order to validate the results, the analytical solution of the problem is provided at four different values of the reduced frequency kR. The *fictitious eigenfrequencies* issue is also addressed with this tutorial, along with the use of the CHIEF method to circumvent it.

1.1 Analytical solution

Let's assume that a point source of unit amplitude is located close to a rigid sphere of radius a. The monopole distance from the sphere center O is r_s. The problem exhibits axial symmetry w.r.t. the axis connecting the sphere center to the source location. Thus, we can obtain the solution in the whole field from its knowledge onto a generic plane passing through the symmetry axis. We can define the polar coordinates, $(r,\, \theta)$ depicted in figure 1.1. The source is located at $\mathbf{r}_s \equiv (r_s, 0)$, whereas a generic point in the field is indicated by $\mathbf{r} \equiv (r, \theta)$. The acoustic potential in the field is the solution of

$$\nabla^2\phi + \kappa^2\phi = \delta(\mathbf{r} - \mathbf{r}_s), \qquad \text{with} \quad \frac{\partial\phi}{\partial r} = 0 \;\; \text{for} \;\; r = a. \tag{1.1}$$

which reads (see, *e.g.*, [2])

$$\phi(r,\theta) = \phi_{inc} + \phi_{sc} = -\frac{e^{j\,kR}}{4\pi R} + \frac{j\,k}{2\pi}\sum_{n=0}^{\infty}\left(n + \frac{1}{2}\right)\frac{j_n'(ka)\; h_n(kr_s)}{h_n'(ka)}\; h_n(kr)\; P_n(cos\theta) \tag{1.2}$$

where h_n and j_n are the spherical Hankel and Bessel functions of the first kind, respectively, P_n is the Legendre polynomial of order n, and $R = \|\mathbf{r} - \mathbf{r}_s\|$. Equation 1.2 is used to

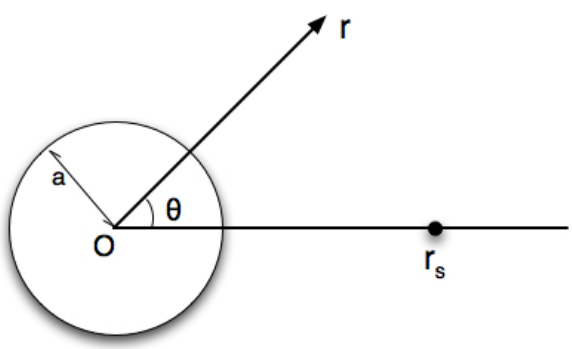

Figure 1.1: Polar coordinates system.

calculate the solution at a circle of microphones located at a distance of $1.5a$ from the centre of the sphere, for $ka = \omega\; a/c = 1, 2, 4, \pi$, with $r_s = 3$. Note that $ka = \pi$ represents the

© U. Iemma & V. Marchese

first eigenfrequency of the interior problem inside the sphere with homogeneous Dirichlet boundary conditions (sound–soft), so the CHIEF regularization technique will be used.

1.2 Files

The files provided with this tutorial are under

`acousto_distribution_path/tutorials/Sphere_Monopole`

and are listed below.

Name	Content
`sphere_source.cfg`	Configuration file for `AcouSTO` built–in pre–processor
`sphere_source_gmsh.cfg`	Configuration file for `Gmsh` geometry
`acousto.sources`	Monopole position and intensity file in `AcouSTO` native format
`acousto.mics1.5.mesh`	Circle of microphones at 1.5 m
`acousto.chief.mesh`	CHIEF points coordinates
`exact_solutions_at1.5`	folder containing analytical solutions at various ka
`gmsh_geom_meshes`	folder containing `Gmsh` files
`compare.gpl`	`gnuplot` script to compare solutions (just change the variable `jobname`)

1.3 Setting up

In this section, the most relevant aspects of the configuration file setup are described. We will first analyze the use of the simple `AcouSTO` built–in functionalities and then what an be done with the `Gmsh` pre–processor.

1.3.1 Using the built–in `AcouSTO` pre–processor

The sphere is one of the simple geometries included in the `AcouSTO` geometry pre–processor. The panels generated by `AcouSTO` on the spherical surface are built on the basis of a parallels/meridians partition, and for this reason some care must be taken to make the discrete geometry be compatible with the axial symmetry of the problem. The sections of the configuration file `sphere_source.cfg` where the geometry is defined are

```
modgeom={
```


© U. Iemma & V. Marchese

```
 active = 1;
 geoms = ["sph"];
 mics_file = "acousto.mics1.5.mesh";
 nmics = 100;
 chief_file = "acousto.chief.mesh";
 nchief = 2;
};
sph={
  type="sphere";
  radius=1.0;
  segments=12;
  rings=12;
translation={x=0.0; y=0.0; z=0.0;};
rotation={x=0.0; y=-90.0; z=0.0;};
};
```

The geometry of the sphere is portioned into 12 meridians and 12 parallels and rotated around the y axis of 90 degrees. The reason of the rotation is to align the polar axis of the discrete geometry with the x axis, which is the one where the monopole is located.[1] The panels mesh is really coarse ad cannot reproduce correctly the phenomenon only at very low frequencies. Once that the user has familiarized with the problem we strongly suggest to increase the number of elements significantly.

1.3.2 Using `Gmsh`

Using `Gmsh` as geometry pre-processor and mesh generator, the user must first generate the the geometry and then produce the mesh according to the needs of the specific application. The directory `gmsh_geom_meshes` contains two geometry files, for the sphere surface and for the microphones located in the field. Note that the layer of microphones is not used to validate the results against the analytic solution (the file `acoustic.mics1.5.mesh` is supposed to be used for this), but only to produce the field visualization depicted at the beginning of the present chapter.

Also with `Gmsh` , the user must pay particular attention in the generation of the geometry, so as to ensure that the mesh would exhibit the same level of symmetry of the continuous geometry. To do that the file `sphere.geo` is provided. It includes a parametric description of a slice of sphere signed with the x axis. The header of the file is

```
// Gmsh project created on Fri Nov 29 18:46:23 2013
ksymmi = 48;                    // Number of slices
sec = 360/(2*ksymmi);    // Slice amplitude in degrees
```

[1] This choose depend on the need to compare the results with the analytical ones, calculated using a different reference configuration. Obviously, a perfectly equivalent alternative is to leave the sphere un–rotated an locate the source along the z axis.

© U. Iemma & V. Marchese

The user can set the desired level of symmetry, and `Gmsh` will automatically produce a slice of the appropriate amplitude. Figure 1.3 shows the geometry obtained by setting `ksymmi=48` The mesh can be now generated according to the general instructions con-

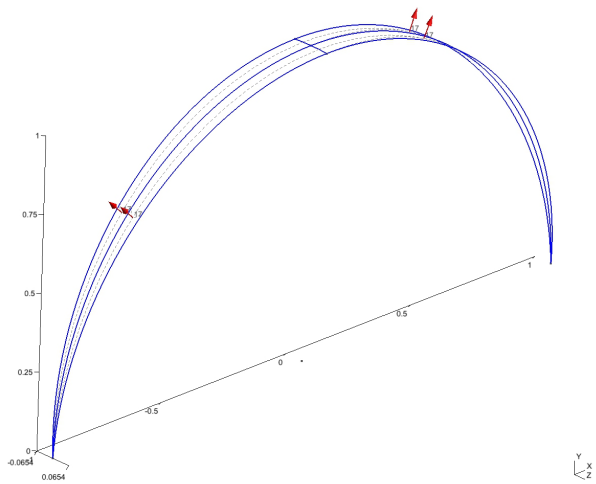

Figure 1.2: Section of sphere geometry for `ksymmi=48`.

tained in the `AcouSTO` user manual and in the `Gmsh` documentation. Just be sure to set a maximum element size compatible with the analysis do you intend to perform. Figure 1.3 depicts the mesh obtained by setting a maximum dimension equal to 0.05. The file

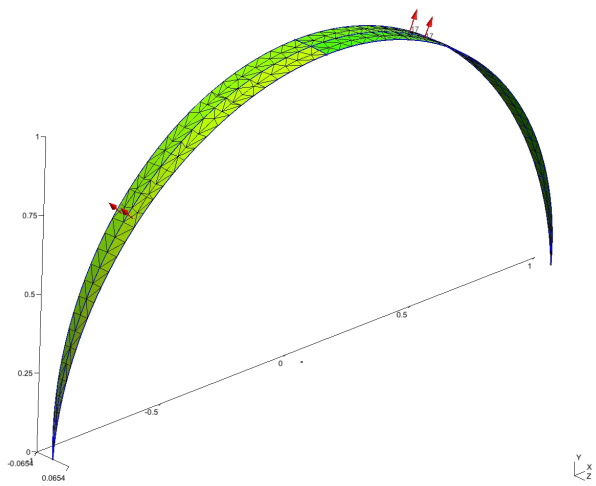

Figure 1.3: Mesh on the section of sphere geometry.

`sphere_source_gmsh.cfg` is ready to import the mesh produced with `Gmsh` . Be sure that the value of `ksymmi` matches the one used in the mesh generation, and to point to the right file

```
runinfo={
```


© U. Iemma & V. Marchese

```
 active = 1;
 title = "JobName";
 owner = "umby";
 ksymmi=48;
 krow  =-1;
 vsound  =343.0;
};

modgeom={
 active = 1;
 geoms = ["gmsphere"];
 chief_file="acousto.chief.mesh";
 nchief=0;
 mics_file = "acousto.mics1.5.mesh";
 nmics=100;
};

gmsphere={
  type="gmsh";
  filename= "./gmsh_geom_meshes/sphere.msh";
  symvec={x=1.0;y=0.0;z=0.0;};
  refpoint={x=0.0;y=0.0;z=0.0;};
};
```

The geometry generated by `AcouSTO` starting from the above example is shown in Figure 1.4, where can be seen how the collocation points are disposed only on the basic slice of the surface.

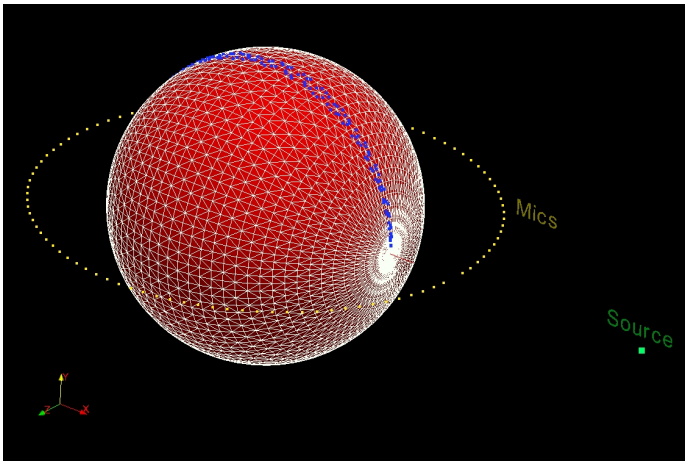

Figure 1.4: Axially-symmetric geometry as generated by `AcouSTO` from `Gmsh` input files. The collocation points (blue) are located only along the basic slice of the sphere, symmetrized by `AcouSTO` around the x–axis.

1.4 Analysis of results

The results of the analysis are presented in this section, using polar plots to represent the total filed at the circle of microphones located at 1.5 radii from the where center. The analytic solution is always represented by a continuous line, whereas markers are used for the `AcouSTO` results. Results are ordered in subsections, where the detailed description of each specific case is given in the figures' captions.

© U. Iemma & V. Marchese

1.4.1 Influence of the reduced frequency, ka

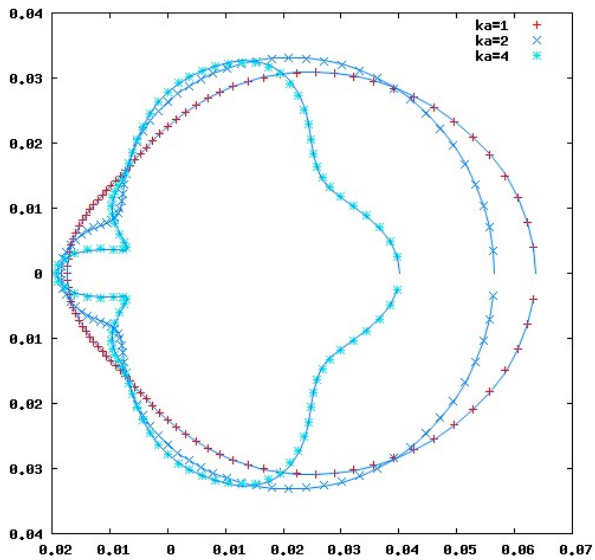

Figure 1.5: Polar plot of the velocity potential amplitude at $r = 1.5$, for $ka = 1, 2, 4$. AcouSTO results (markers) obtained with the built–in geometry pre–processor are compared with the analytical solution (continuos line).

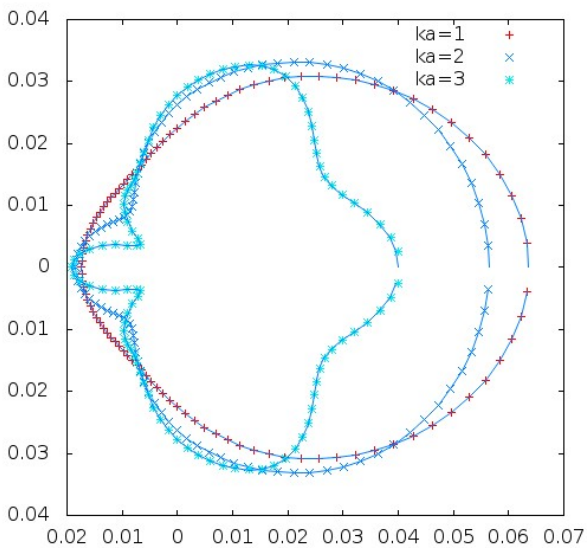

Figure 1.6: Polar plot of the velocity potential amplitude at $r = 1.5$, for $ka = 1, 2, 4$. AcouSTO results (markers) obtained with the `Gmsh` mesh are compared with the analytical solution (continuos line).

© U. Iemma & V. Marchese

1.4.2 Symmetry management

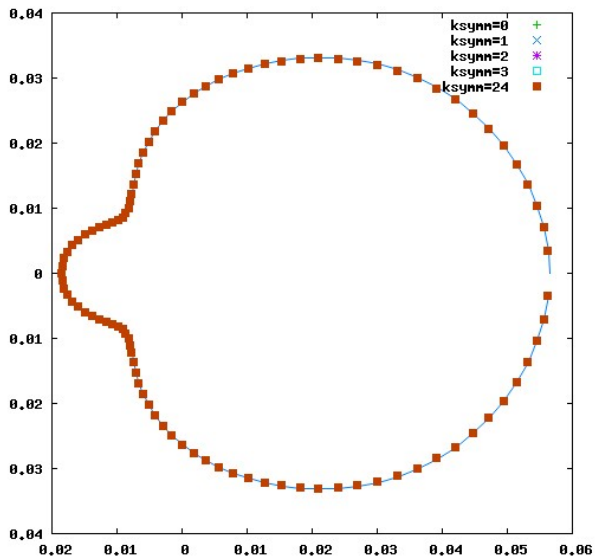

Figure 1.7: Polar plot of the velocity potential amplitude at $r = 1.5$, for $ka = 2$. Assessment of AcouSTO symmetry management for `ksymmi=0,1,2,3,24`.

1.4.3 Primary field formulation

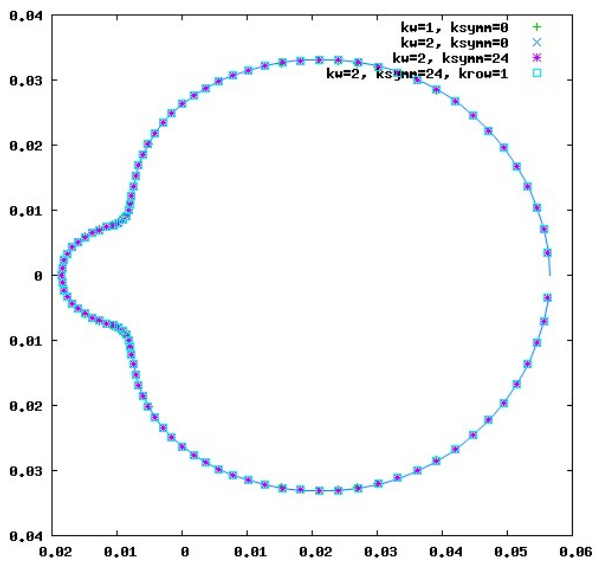

Figure 1.8: Polar plot of the velocity potential amplitude at $r = 1.5$, for $ka = 2$. Assessment of AcouSTO formulations A and B (`knw=1` or `knw=2`, respectively).

© U. Iemma & V. Marchese

1.4.4 Regularization at spurious eigenfrequencies

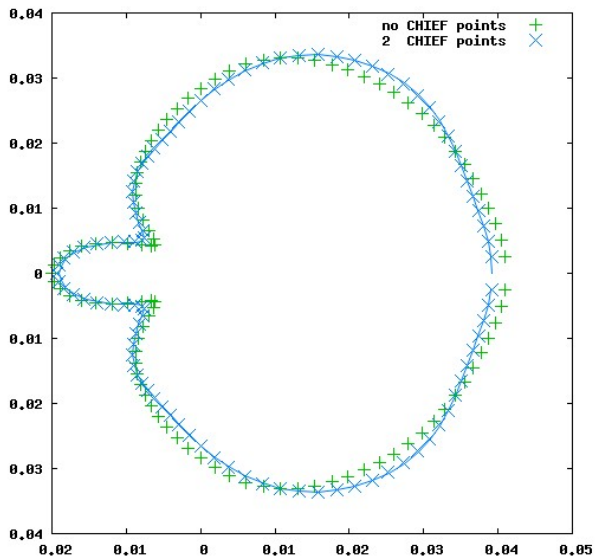

Figure 1.9: Polar plot of the velocity potential amplitude at $r = 1.5$, for $ka = \pi$. CHIEF regularization at a singular frequency with the `AcouSTO` built–in pre–processor. NCHIEF=2, $\mathbf{x}_{ch_1} \equiv (0.0, 0.0, 0.0)$, $\mathbf{x}_{ch_2} \equiv (0.41, 0.2, 0.1)$.

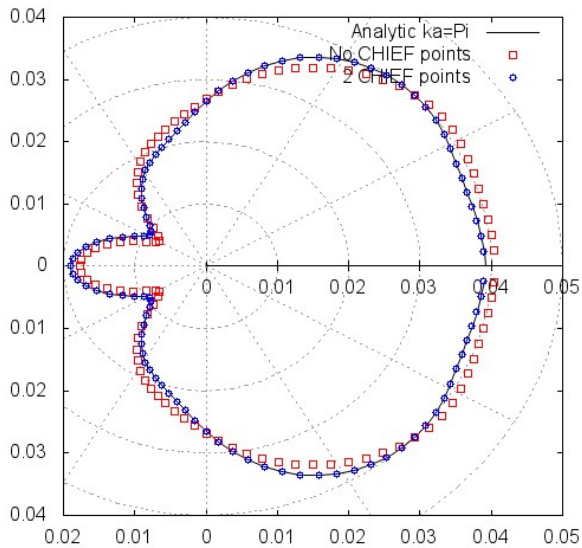

Figure 1.10: Polar plot of the velocity potential amplitude at $r = 1.5$, for $ka = \pi$. Effect of the use of the CHIEF technique with the `Gmsh` mesh. NCHIEF=2, $\mathbf{x}_{ch_1} \equiv (0.0, 0.0, 0.0)$, $\mathbf{x}_{ch_2} \equiv (0.41, 0.2, 0.1)$.

© U. Iemma & V. Marchese

CHAPTER 2

Scattering of a plane wave by an impedance sphere

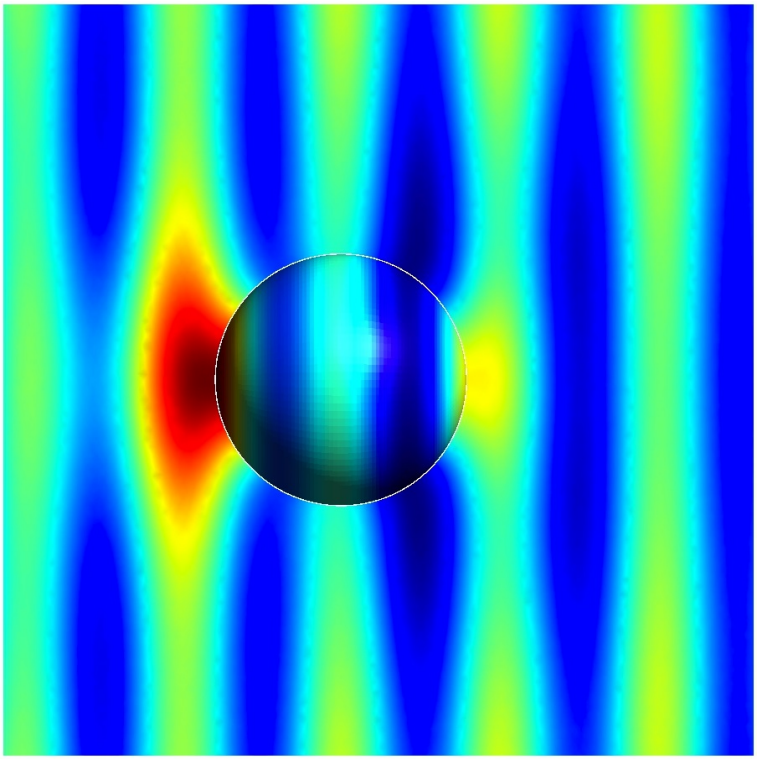

The effect of impedance

Here, the primary field is that produced by an incoming plane wave, moving from the negative side of the x axis. The sphere is impinged onto one of its poles, to keep the discrete problem axially symmetric.

The attention is focused on impedance boundary conditions. The solution is computed for different values of the complex surface impedance $\mathcal{Z}$ of the sphere, using all the possible approaches available in `AcouSTO` . Solution is validated against the analytical one.

2.1 Analytical solution

Referring to the same geometry and coordinates convention used in Section 1.1, the total pressure field induced by a plane wave of unit amplitude,scattered by a sphere of radius a, is (see, *e.g.*, [3])

$$p(r,\theta) = p_{inc} + p_{sc} = e^{jkrcos\theta} - \sum_{n=0}^{\infty} (2n+1)\ j^n P_n(cos\theta) \frac{j_n'(ka) + j\,\beta j_n(ka)}{h_n'(ka) + h\,\beta j_n(ka)}\ h_n(kr) \quad (2.1)$$

where h_n and j_n are the spherical Hankel and Bessel functions of the first kind, respectively, P_n is the Legendre polynomial of order n, and $\beta = \varrho\, c_0/\mathcal{Z}$. Equation 2.1 is used to calculate the solution at a circle of microphones located at a distance of $1.5a$ from the centre of the sphere, for $ka = \omega\ a/c = 1, 2, 4$, and $\mathcal{Z} = 100.0 + j\,0.0$ and $\mathcal{Z} = 1.0 + j\,0.0$.

2.2 Files

The files provided with this tutorial are under

`acousto_distribution_path/tutorials/Imped_Sphere_PlaneWave`

and are listed below.

It is worth noting that the multiple `lambda`–files are required because a wall impedance constant with frequency corresponds to a frequency-dependent Λ matrix.

2.3 `AcouSTO` solution using the *impedance body* option

When the surface of the scatterer is characterized by a uniform wall impedance, the option of *impedance body* can be used. This is the simpler way to perform a single–frequency run in such a case. Indeed, it sufficient to provide a negative value for `nimped` in the config file, and `AcouSTO` automatically associates the value of $\mathcal{Z}$ to al the boundary panels. The relevant section of the config file would appear as

© U. Iemma & V. Marchese

Name	Content
sphere_pw.cfg	Configuration file for AcouSTO built–in pre–processor
acousto.planw	Plane wave definition file in AcouSTO native format
acousto.mics1.5.mesh	Circle of microphones at 1.5 m
impedXXX.panels	files containing the definition of panel impedance
lambda_kaX.panels	custom boundary conditions λ files for various frequencies
gamma.panels	custom boundary conditions γ file
exact_sol_at1.5	folder containing analytical solutions at various ka and $\mathcal{Z}$

```
modsol={
 active=1;
 nimped=-1;
 impedance_real=100.0;
 impedance_imag=0.0;
 ...
 ...
```

Figure 2.1 shows the solution obtained using this approach at different values of the frequency for $\mathcal{Z} = 100.0 + j0.0$. It is important to notice that no regularization is required at $ka = \pi$ because of the impedance boundary conditions (see [5] for details). The effect of the value of $\mathcal{Z}$ is shown in Figure 2.2.

2.4 AcouSTO solution using an impedance file

Although not strictly necessary in this case, because of the uniform properties of the entire boundary, impedance boundary conditions can be given also through an impedance file containing the value of the complex impedance for each boundary element. The files impedXXX.panels contain 48 lines (one for each element of the base slice of the sphere). The content of the imped100.panels file looks like

```
 1  100.0  0.0
 2  100.0  0.0
 ...
 48  100.0  0.0
```


© U. Iemma & V. Marchese

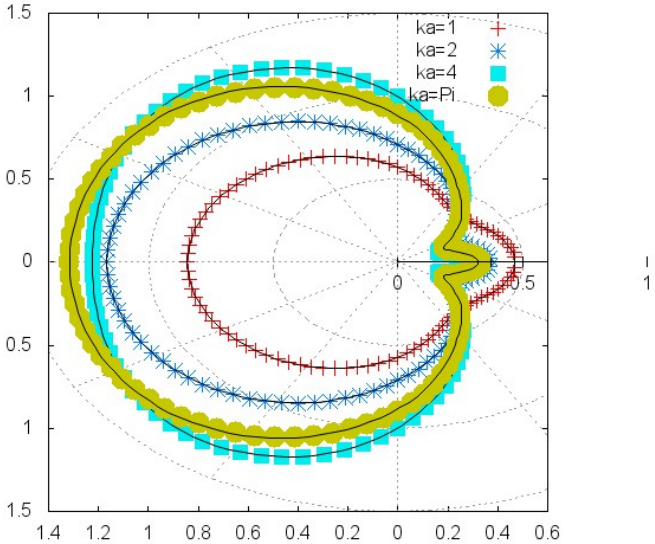

Figure 2.1: Directivity pattern of the total field at a $1.5a$ from the sphere center. Markers indicates the AcouSTO solution for $ka = 1, 2, 4, \pi$. Continuos black lines depict the analytical solution obtained with Eq. 2.1. Input provided with the *impedance body* option.

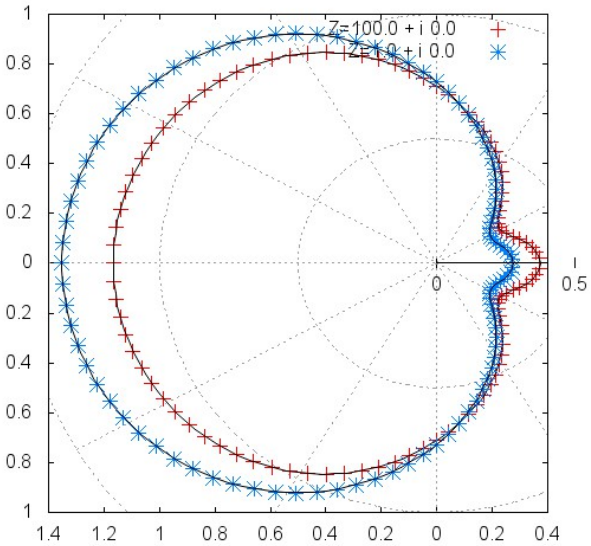

Figure 2.2: Directivity pattern of the total field at a $1.5a$ from the sphere center. Markers indicates the AcouSTO solution for $Re(\mathcal{Z}) = 100$ and $Re(\mathcal{Z}) = 1$. Continuos black lines depict the analytical solution obtained with Eq. 2.1. Input provided with the *impedance body* option.

The corresponding portion of the config file is

© U. Iemma & V. Marchese

```
modsol={
 active=1;
 imped_file = "imped100.panels";
 nimped=48;
 ...
 ...
```

The solution obtains with this approach is presented in Figure 2.3. Obviously, the solution obtained is exactly equivalent to that observed in the previous Section.

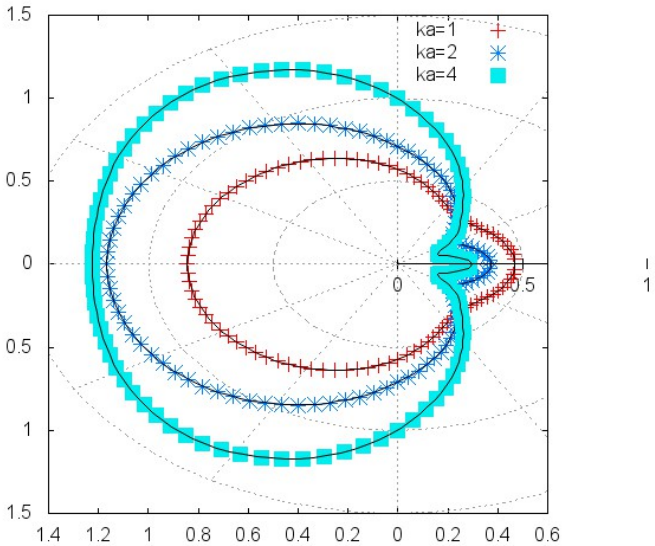

Figure 2.3: Directivity pattern of the total field at a $1.5a$ from the sphere center. Markers indicates the AcouSTO solution for $ka = 1, 2, 4, \pi$. Continuos black lines depict the analytical solution obtained with Eq. 2.1. Input through impedance file.

2.5 AcouSTO solution using custom boundary conditions

The third approach available in AcouSTO to define the boundary conditions is what we call *custom* bounder condition. It is the most general approach allowing the user to define any kind of boundary conditions from the general form

$$\gamma(\mathbf{x},\kappa)\,\tilde{\varphi}(\mathbf{x},\kappa) + \lambda(\mathbf{x},\kappa)\,\frac{\partial\tilde{\varphi}(\mathbf{x},\kappa)}{\partial n} = \tilde{f}(\mathbf{x},\kappa) + \tilde{\mathbf{g}}(\kappa)\cdot\mathbf{n}(\mathbf{x}), \qquad \text{for } \mathbf{x}\in\partial\mathcal{V} \tag{2.2}$$

In case of an impedance boundary, the values of the complex coefficients appearing in Eq. 6.12 can be obtained from the definition of point impedance (the surface is assumed to be

© U. Iemma & V. Marchese

locally reacting)

$$\mathcal{Z} = \frac{\tilde{p}}{\mathbf{v} \cdot \hat{\mathbf{n}}_{in}} \tag{2.3}$$

where $\mathbf{n}_{in}$ is the unit vector pointing into the boundary. To derive their specific form, e need to give a physical interpretation to the function $\tilde{\varphi}$. In Section 2.5 of the User Manual, we assumed that $\tilde{\varphi}$ is the acoustic velocity potential. On the contrary, we here write the same equation for the acoustic pressure perturbation (dropping the $\sim$ for notational simplicity)

$$\gamma\, p + \lambda \frac{\partial p}{\partial n} = \tilde{f} + \tilde{\mathbf{g}} \cdot \mathbf{n} \tag{2.4}$$

Recalling the linearized Bernoulli theorem and the orientation of the domain boundary, it an be easily seen that

$$\mathbf{v} \cdot \hat{\mathbf{n}}_{in} = -\mathbf{v} \cdot \hat{\mathbf{n}} = -\nabla\varphi \cdot \hat{\mathbf{n}} = -\frac{\partial \varphi}{\partial n} = \frac{1}{j\,\varrho\,\omega}\frac{\partial p}{\partial n} \tag{2.5}$$

Substituting into Eq. 2.3 and comparing with 2.6, we obtain, on each panel,

$$f = 0,\ \mathbf{g} \equiv (0,0,0),\ \gamma = 1,\ \lambda = \frac{\mathcal{Z}}{j\,\varrho\,\omega} \tag{2.6}$$

As a consequence, the Λ matrix depends on frequency. The content of the config file is

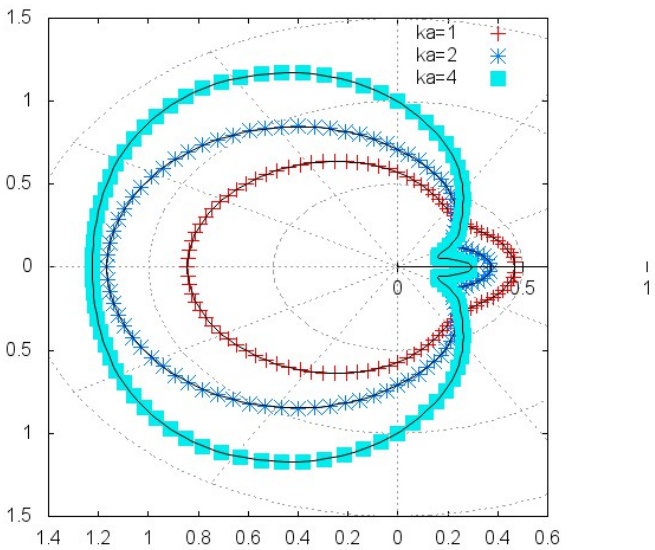

Figure 2.4: Directivity pattern of the total field at a $1.5a$ from the sphere center. Markers indicates the AcouSTO solution for $ka = 1, 2, 4, \pi$. Continuos black lines depict the analytical solution obtained with Eq. 2.1. Custom boundary conditions.

```
modsol={
 active=1;
```


© U. Iemma & V. Marchese

```
custombc=1;
bc_gamma_file="gamma.panels";
bc_lambda_file="lambda_ka2.panels";
bc_func_file="func.panels";
bc_g_file="g.panels";
planw_file="acousto.planw";
nplanw=1;
knw=2;
rho=1.21;
minsig=0.0;
maxsig=0.0;
nsig=1;
minfreq=109.18;
maxfreq=218.36;
nome = 1;
 ...
...
```

Be sure to provide the value of the frequency corresponding to the Λ matrix chosen (in this case, $ka = 2 \Rightarrow 109.18$ Hz. The results are depicted in Fig. 2.4. Also in this case the solution is in perfect agreement with the analytical one.

© U. Iemma & V. Marchese

CHAPTER 3

Engines' shielding effect of an aircraft model in static conditions

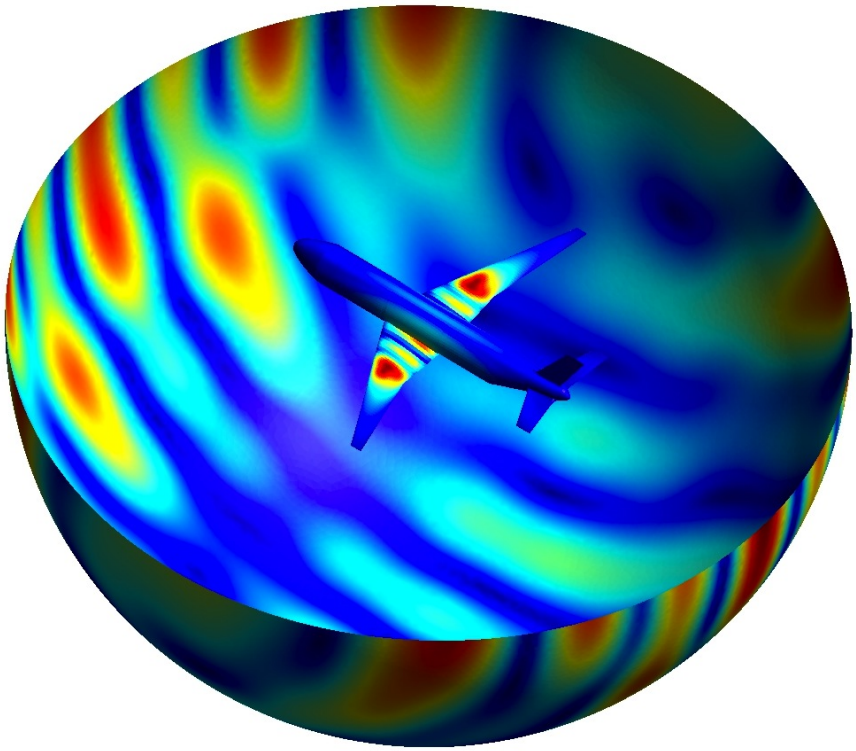

How bodies mask noise

3.1 Description

This tutorial deals with the evaluation of the scattering effect produced by an aircraft model on the field generated by two monopoles. This analysis can be seen as a rough simplification of the effect on noise propagation of an unconventional over–the–wing installation of the engines.

It is clearly only an exercise, because the strong directivity of the actual noise sources is not taken into account at all. Nevertheless, with a careful choice of the location of the monopoles and of their intensity, such an analysis can be used to derive digital filters to be applied to a real spectrum to estimate the installation loss.

The analysis does not take into account the aircraft speed. This possibility is currently available in an unreleased version of `AcouSTO` , and will be release to the public most likely with `AcouSTO` v2.0.

3.2 Files

The files provided with the tutorial are listed below

Name	Content
`aircraft.cfg`	Configuration file
`aircraft_15345N_15028E.nodes`	File of the aircraft geometry produced with an in–house developed external tool in native `AcouSTO` *nodes* format. Geometry is made of 15345 nodes and 15028 quadrilateral elements. The size of the aircraft is scaled down by the factor 0.2.
`aircarft.sources`	Monopoles file in `AcouSTO` native format.
`microphones.geo`	`Gmsh` geometry description file to produce a planar layer of microphones.
`microphones_sphere.geo`	`Gmsh` geometry description file to produce a spherical layer of microphones.
`microphones_size0.4_z10.msh`	`Gmsh` microphones planar mesh obtained with the `.geo` file, located 10 meters below the aircraft
`microphones_size0.4_sphere.msh`	`Gmsh` microphones spherical mesh obtained with the `.geo` file, 10 meters radius.

© U. Iemma & V. Marchese

3.3 How to use it

This tutorial comes with a fixed geometry of the scatterer, so the user has no possibility to modify it.[1]

The figure use in the first page of the present chapter has been obtained using the settings included in the provided files. Note that the mesh of the aircraft is quite coarse, and the analysis at frequencies higher than 350 Hz cannot be considered accurate.

The `Gmsh .geo` files can be used to modify the shape, the extent and the position of the layer of microphones used to monitor the field. The header of the two files include self–explanatory parameters that can be modified by the user. The procedure to produce a miss mesh compatible with `AcouSTO` is the following

1. Load the file of interest into `Gmsh` using the `File>Open` menu.
2. Select the `Edit file` options in the left menu and modify the initial parameters as desired. Save the file and select the `Reload file` option from the same menu.
3. Open the `Tools>Options` menu and the `Mesh>General` submenu in the opened window. decide a maximum size for the element. As a rule–of–thumb to have a nice visualization of the field you can use one fifth of the wavelength. Note that this choice **does not affect the accuracy of the solution** (which is related to the boundary mesh size), but only the quality of the field visualization.
4. Select the `Mesh>1D` option in the left menu to build the partition of the surface edges.
5. Select the `Mesh>2D` option in the left menu to build the surface mesh.
6. Save the mesh in `Gmsh` format, `.msh`.

In the distribution, one spherical mesh and one planar mesh are included. Both have a maximum element size of 0.4 m.

Now you can modify the config file with the name of the mics mesh produced and run the code with the command

```
mpiexec -np N /path_to_acousto/acousto -f aircraft.cfg
```

where `N` is the number of processes. On a MacPro equipped with 2×2.26 GHz, Quad-Core Xeon, the run takes 110 seconds to be completed, with $N = 16$ (hyper–threading).

[1] Actually, one could import the `AcouSTO` output in wrl or vtk format and try to hack the geometry in some way using Blender or any othe 3D modeler capable to import those formats. But this is another story, we are not interested in ...

© U. Iemma & V. Marchese

The user can play with the config settings to see what are the effects on the solution. A possible list of tests is the following.

- Being the sources two simple monopoles, the two formulations for the primary field treatment can be used, switching `knw` from 1 to 2.
- Changing the position of the sources can give an idea of the effect of installation on the noise propagation.
- Also the frequency can be changed to see how deeply the scattering pattern is affected.

3.4 Results

The results obtained with the mesh provided with the `AcouSTO` distribution are summarized in this section. Specifically, Figures 3.1 to 3.4 show the SPL at the microphones hemisphere for four frequencies, from 150 to 750 Hz. The effect of frequency on the masking effect is evident. The lowest frequency analyzed corresponds to a wavelenght of 2.82 meters, which is comparable to the dimensions of the aircarft model. In this condition, the scattering of the incident wave is dominant. The interaction of the fields induced by the two sources yields a strip of increased noise along the symmetry line with a limited shielding effect ahead of the fuselage nose. As the frequency increases the shadow produced by wings and fuselage on the monitoring hemisphere becomes clear, as an effect of the reduced wave scattering for shorter wavelenghts and the increase upward reflection of the wings. In addition, the reflection induced by the fuselage enhances the effect of noise amplification on the aircarft plane. The difference between maximum and minimum noise levels increases from roughly 15 dB at 350 Hz to about 25 dB at 750 hz.

It is important to emphasize that this execercise doesn't take into account the effect of motion of sources and aircraft. This effect may significantly modify the directivity of propagation and yields to completely different noise patterns on the observation hemisphere. The effect of moving sources and boundaries is currently available only in an internal version of the code and will be released in one of the future versions.

© U. Iemma & V. Marchese

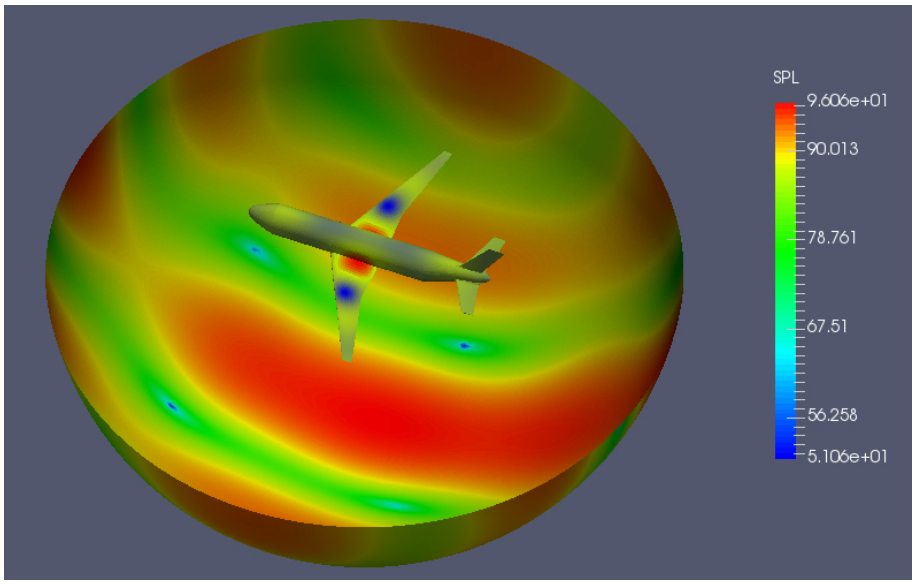

Figure 3.1: Real part of the total field on the aircraft surface and SPL on the microphones hemisphere at 150 Hz.

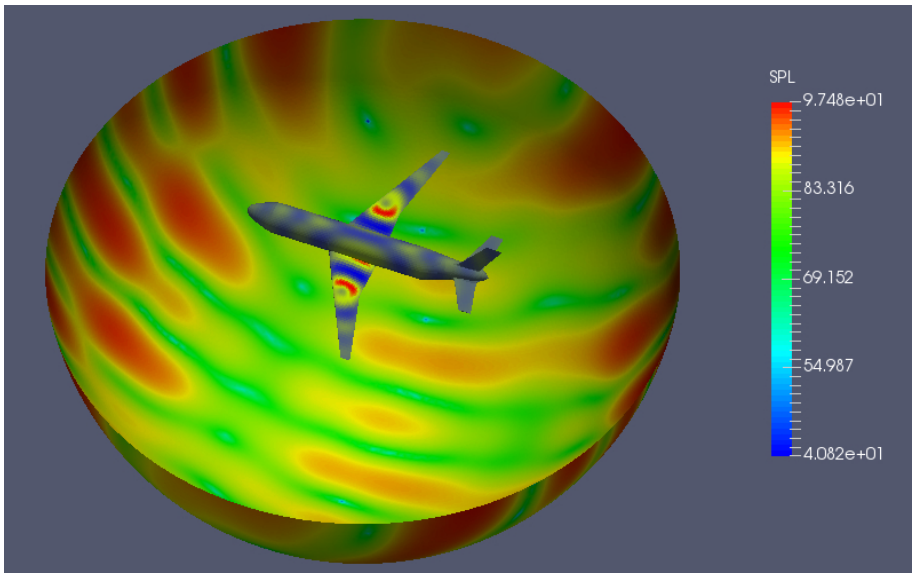

Figure 3.2: Real part of the total field on the aircraft surface and SPL on the microphones hemisphere at 350 Hz.

© U. Iemma & V. Marchese

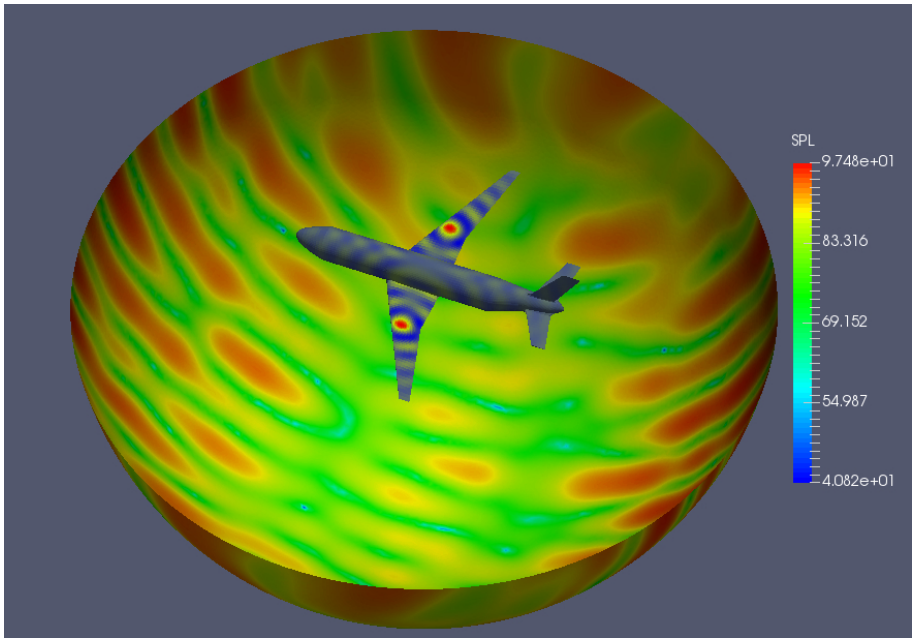

Figure 3.3: Real part of the total field on the aircraft surface and SPL on the microphones hemisphere at 550 Hz.

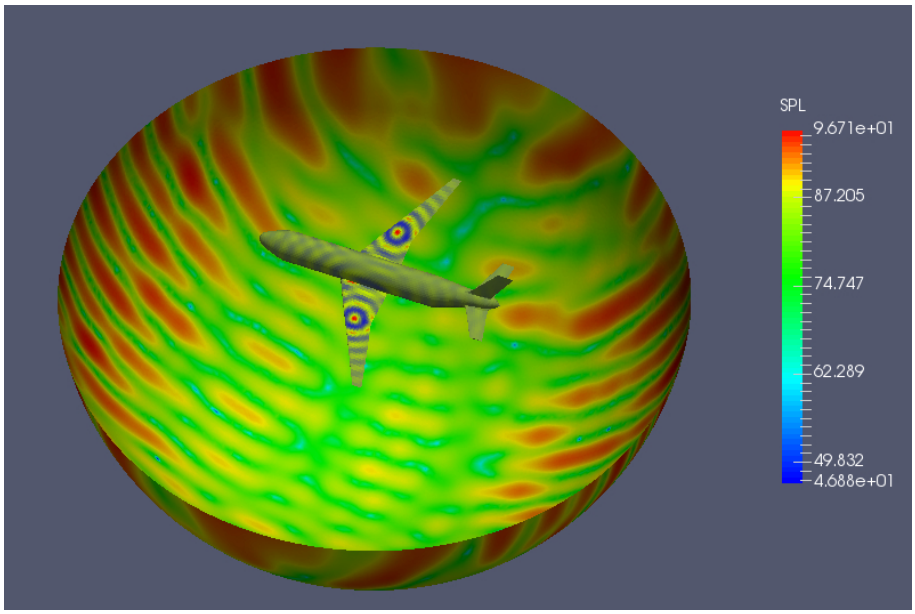

Figure 3.4: Real part of the total field on the aircraft surface and SPL on the microphones hemisphere at 750 Hz.

© U. Iemma & V. Marchese

CHAPTER 4

Frequency response of a $E_\flat$–tuned natural trumpet

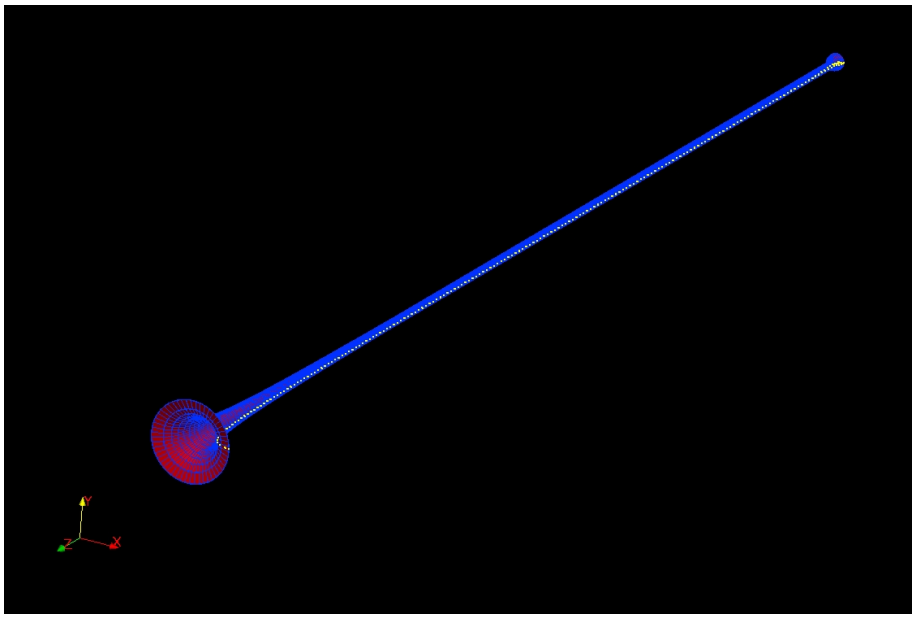

Learn about frequency response with some music

This tutorial is dedicated to the multi-frequency analysis, typically used to simulate the frequency response of an acoustic device. The application chosen to describe this kind of jobs is the evaluation of the acoustic response of a natural trumpet.

Specifically, the spectrum of the acoustic pressure at three microphones located close to the output section of the instrument flare is evaluated in the frequency range $0 \leq f \leq 1000$ Hz.The acoustic field is induced by a uniform radiation of the panels corresponding to the input section of the mouthpiece. The radiation of the input section has complex amplitude $\tilde{f} = 1$ in the whole frequency range considered.

4.1 Files

The files provided with this tutorial are under

`acousto_distribution_path/tutorials/Brass_FreqResponse`

and are listed below.

Name	Content
`brass_fresp.cfg`	Configuration file
`acousto.mics.dat`	Microphones in the field
`Brass.nodes`	geometry of the trumpet in `AcouSTO` *nodes* format
`acousto.custombc.XXXX.dat`	Files containing custom boundary conditions
`equal_temp_freqs`	Frequencies of the equal tempered scale, for comparison and validation of results.

4.2 How to use it

The files provided with the tutorial are ready to be used in `AcouSTO` . The user with a working `AcouSTO` installation should be able to run the test with the standard command.

In this Section, we summarize the specific issues that the user should be aware of when performing frequency response analysis.

1. Considering that the number of frequencies analyzed could be very high (512 in the example, but often much more are needed) the number of file produced could be also very high. Remember to activate only the output format you really need.

© U. Iemma & V. Marchese

2. In this kind of analysis it is extremely convenient to adopt the pre–calculation of integral coefficients by setting

   `pre_calculated_coefs=1;`

   or by omitting the entry from the config file (the variable defaults to 1, for backward compatibility). Indeed, the integration over the boundary panels does not depend on frequency and thus is calculated only once. Anyway, be sure that your system has enough memory to store them. Remember also to activate the coefficients evaluation modules

```
modcoefac = {
   active              = 1;
};
modcoemic = {
   active              = 1;
};
```

3. The frequency response of the trumpet is obtained assuming that at the mouthpiece input section the condition is given by

$$\frac{\partial \varphi}{\partial n} = 1.0, \qquad \text{for } \; f_{min} \leq f \leq f_{max} \tag{4.1}$$

   This boundary condition is imposed using the custom declaration with (see `AcouSTO` User Manual)

$$\tilde{f} = 1.0, \;\; \lambda = 1.0, \;\; \gamma = 0.0, \;\; \mathbf{g} \equiv (0.0, 0.0, 0.0) \tag{4.2}$$

   The geometry was built using a single panel for the input section, so, only one record is included in the custom b.c. files.

4. The frequency response is written on files only for the collocation points and microphones indicated in the `modsol` section of the config file.

4.3 Results

The results of the analysis performed in the range 40-1000 Hz is presented in Figure 4.3 for the three microphones closest to the trumpet output section. The response exhibits 7 peaks in the frequency range analyzed, corresponding to the equal tempered pitches indicated along the abscissae. As can be seen, the fourth peak corresponds to $E_{\flat_4}$, which represents the tuning of the instrument.

4.3.1 Input impedance of the instrument

An important property of a musical pipe is the complex input impedance, defined as

$$Z_{in}(\omega) = \frac{\tilde{p}_{in}(\omega)}{\tilde{u}_{in}(\omega)} \tag{4.3}$$

© U. Iemma & V. Marchese

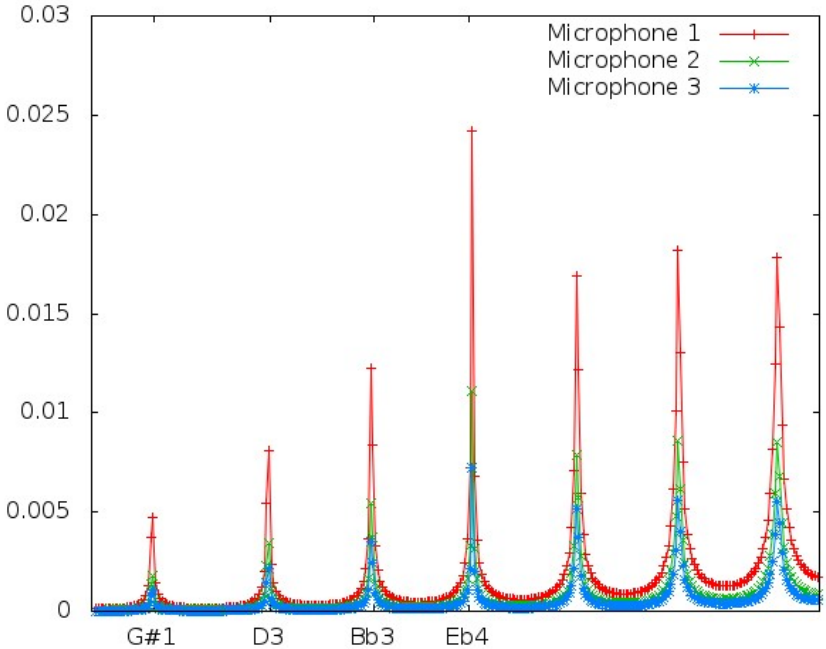

where $\tilde{u}_{in}$ and $\tilde{p}_{in}$ represent the pressure and the flow at the input section of the pipe, respectively. Interpreting the `AcouSTO` analysis performed in terms of acoustic velocity potential, the boundary condition yields

$$\tilde{u}_{in} = \nabla\tilde{\varphi} \cdot \mathbf{n}_{in} = \frac{\partial \varphi}{\partial n} = 1, \qquad \text{for } \mathbf{x} \in \mathcal{S}_{in} \tag{4.4}$$

Thus, recalling the Bernoulli theorem, the input impedance spectrum can be computed from the solution $\tilde{\varphi}$ as

$$Z_{in}(\omega) = -j\,\omega\,\rho\,\tilde{\varphi}_{in}(\omega) \tag{4.5}$$

The input impedance spectrum can be easily obtained with `AcouSTO` setting

```
freq_resp_cnt = [1];
```

in the `modsol` section of the config file.

© U. Iemma & V. Marchese

CHAPTER 5

A simple radiating box

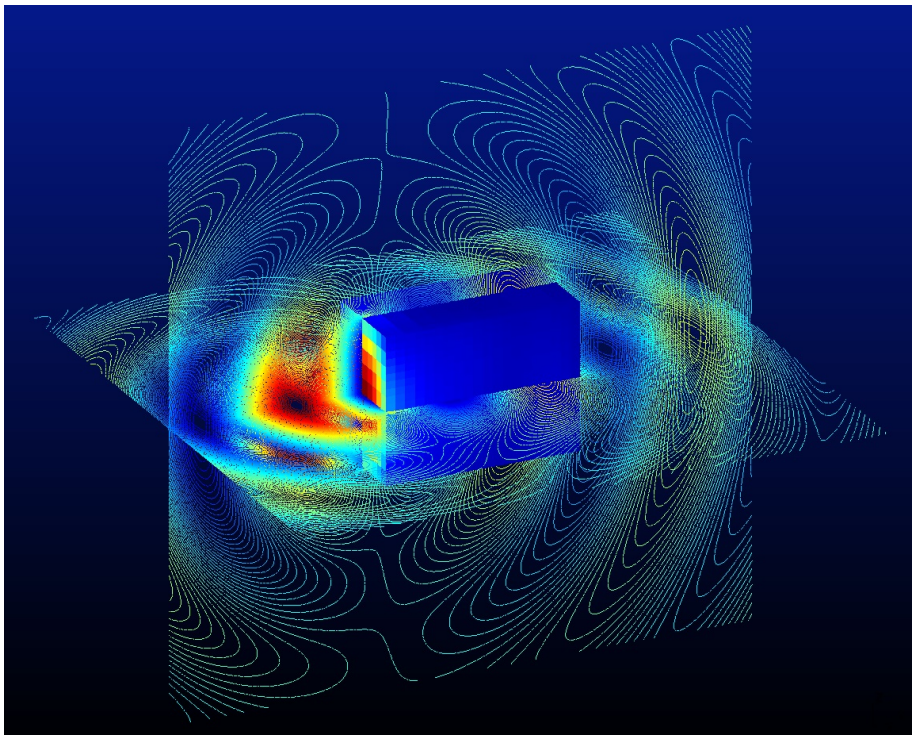

Learn how to handle multiple geometries

Here, we familiarize with the use of multiple geometries with `AcouSTO` . Specifically, a simple rectangular box is built using the built–in module `plate`. Six plates are specified to form each face of the box by translation and rotation. One of box's faces radiates uniformly. On all the others sound–hard conditions are applied. The field is reconstructed on two planes of microphones, orthogonal to the radiating wall.

5.1 Files

The files provided with this tutorial are under

`acousto_distribution_path/tutorials/Radiating_Box`

and are listed below.

Name	Content
`box.cfg`	Configuration file
`mics.geo`	Microphones layer geometry (`Gmsh geo` file)
`mics.msh`	Microphones mesh (`Gmsh msh` file)
`radiant.panels`	list of radiating panels

5.2 Geometry generation and simulation

The box dimensions are $1 \times 1.5 \times 2$ and one of its 1×1.5 faces radiates uniformly. The geometry of the boundary is entirely generated using the `AcouSTO` built–in module `plate`. Six geometry blocks of type `plate` are used, each one suitably translated and rotated to produce eventually a closed box. The geometry section of the config file is

```
modgeom={
 active = 1;
 geoms = ["pl1","pl2","pl3","pl1b","pl2b","pl3b"];
 mics_file = "mics.msh";
};

pl1={
  type="plate";
  l1=1.0;
  l2=2.0;
  n1=10;
  n2=10;
translation={x=0.0; y=0.0; z=0.75;};
rotation={x=0.0; y=0.0; z=0.0;};
};

pl2={
  type="plate";
  l1=1.5;
  l2=2.0;
  n1=20;
  n2=20;
translation={x=0.5; y=0.0; z=0.0;};
rotation={x=0.0; y=90.0; z=0.0;};
```


© U. Iemma & V. Marchese

```
};

pl3={
  type="plate";
  l1=1.0;
  l2=1.5;
  n1=10;
  n2=10;
translation={x=0.0; y=-1.0; z=0.0;};
rotation={x=90.0; y=00.0; z=0.0;};
};

pl1b={
  type="plate";
  l1=1.0;
  l2=2.0;
  n1=10;
  n2=10;
translation={x=0.0; y=0.0; z=-0.75;};
rotation={x=0.0; y=180.0; z=0.0;};
};

pl2b={
  type="plate";
  l1=1.5;
  l2=2.0;
  n1=20;
  n2=20;
translation={x=-0.5; y=0.0; z=0.0;};
rotation={x=0.0; y=-90.0; z=0.0;};
};

pl3b={
  type="plate";
  l1=1.0;
  l2=1.5;
  n1=10;
  n2=10;
translation={x=0.0; y=+1.0; z=0.0;};
rotation={x=-90.0; y=00.0; z=0.0;};
};
```

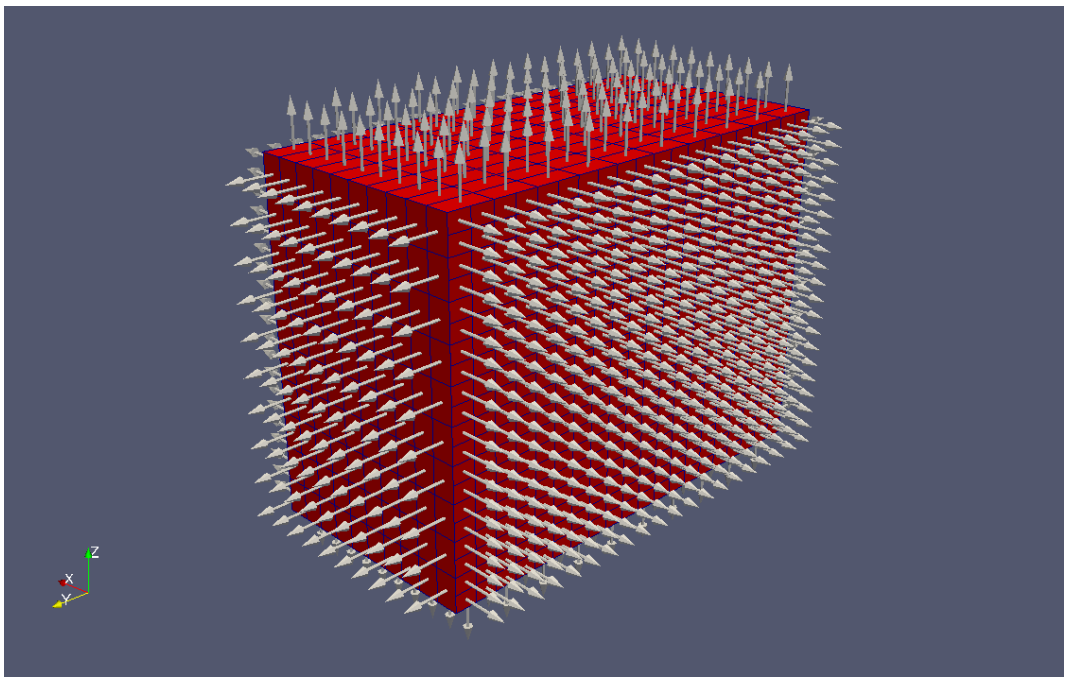

Figure 5.1: Final geometry with normal vectors at panels.

There two aspects that must be taken into account when building complex geometries

© U. Iemma & V. Marchese

using the built–in blocks

1. the procedure that `AcouSTO` uses to transform the geometries is the following
   (a) scaling
   (b) rotation around x axis
   (c) rotation around y axis
   (d) rotation around z axis
   (e) translation

   Keep in mind the transformation sequence when building the config file.

2. When a closed geom is built assembling open surfaces (such in this case) the rotation sign controls the direction of the normal vectors at the boundary elements. Always check the unit normal sign using the `vtk` file. Figure 5.1 shows how the correct geometry would look like.

The simulation results are shown in Figures 5.2 and 5.3 as the real part and absolute value of the acoustic pressure, respectively.

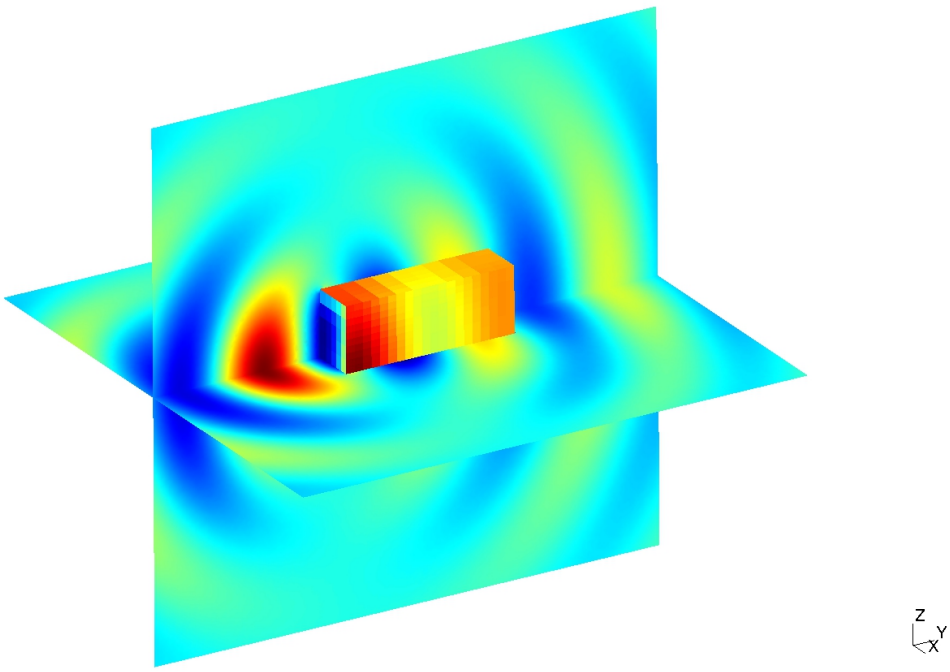

Figure 5.2: Real part of the acoustic field on the box and in the surrounding field.

© U. Iemma & V. Marchese

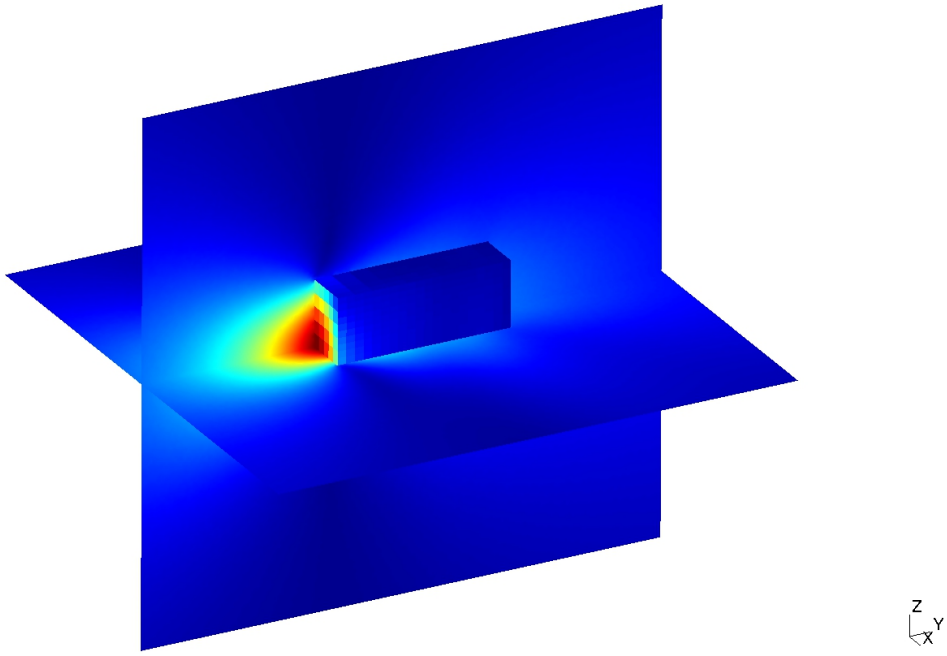

Figure 5.3: Absolute value of the acoustic field on the box and in the surrounding field.

© U. Iemma & V. Marchese

CHAPTER 6

Just a bit of room acoustics

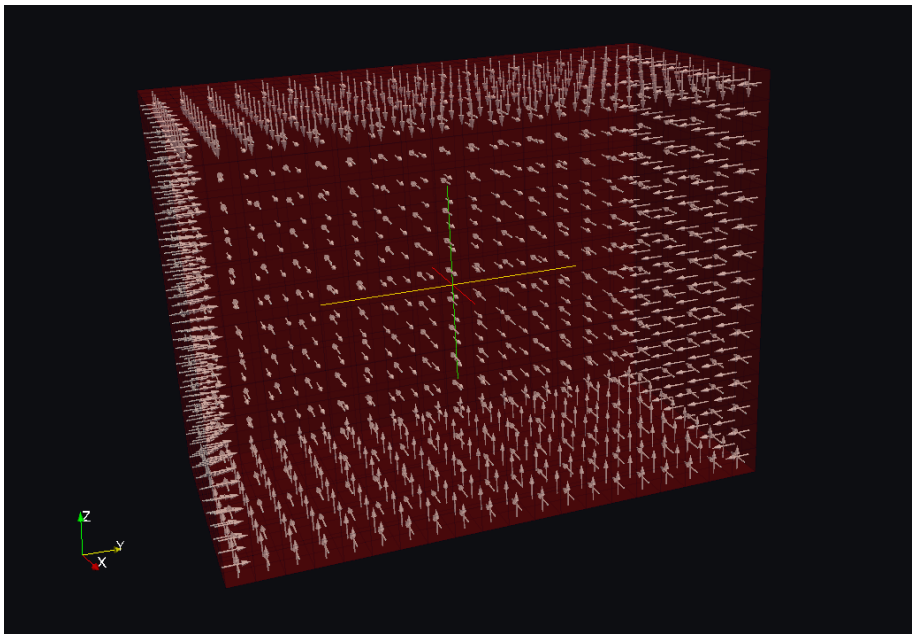

Learn how to handle noise in enclosures

AcouSTO can also do interior (or room) acoustics. Obviously, when the domain of propagation is finite, part of the advantages of the BEM with respect to FEM and other *field methods* is lost. Nevertheless, in some case it remains a reliable, simple and fast tool of analysis. In the present tutorial, we address the setup of a simple problem of interior acoustics using the same box of the previous chapter, but with reversed orientation of the boundary. A simple point source is located inside, and the frequency response is evaluated at a monitoring point. First, we analyse the frequency response of the cavity with sound–hard walls using the same approach used for the brass in Chapter 4: the frequency range of interest is spanned with a monopole source of unit amplitude (real), and the absolute value of the total filed is plotted at the monitoring microphone. The response peaks corresponding to the eigenfrequency of the cavity are compared to their analytical values, and some of the related eigenmodes are plotted on a layer of microphones.

Then, one of the walls is assumed to be covered with a layer of sound absorbing material with a known, frequency–independent absorption coefficient, and a source with a given power output is assumed to be placed inside the room. The values of the complex wall impedance and source amplitude are derived, and the simulation is performed using all the options available in AcouSTO .

6.1 Files

The files provided with this tutorial are under

`acousto_distribution_path/tutorials/Room_Acoustics`

and are listed below.

Name	Content
`room.cfg`	Configuration file
`acousto.sources`	Source location and amplitude
`monitor.mic`	Internal microphone for frequency response evaluation
`mics.geo, mics.msh`	`Gmsh` file for internal layers of microphones (single frequency analysis)
`imped.panels`	Impedance panels for `imped_file` directive
`gamma.panels, lambda.panels`	Boundary condition files for `custombc` input scheme

© U. Iemma & V. Marchese

6.2 Response with sound–hard walls

The acoustic response of a rectangular room with sound–hard walls can be analysed in terms of fundamental modes of vibrations. They can be easily calculated analytically for this simple test case. The eigenfunctions of a rectangular cavity with dimensions L_x, L_y, L_z are given by

$$\Psi_{ijk}(\mathbf{x}) = A\, cos\left(\frac{i\,\pi\,x}{L_x}\right)\, cos\left(\frac{j\,\pi\,y}{L_y}\right)\, cos\left(\frac{k\,\pi\,z}{L_z}\right) \tag{6.1}$$

where the indices $0 \leq i, j, k \leq \infty$ (not all zero simultaneously) and A is an arbitrary constant. The corresponding eigenfrequencies in Hz are given by

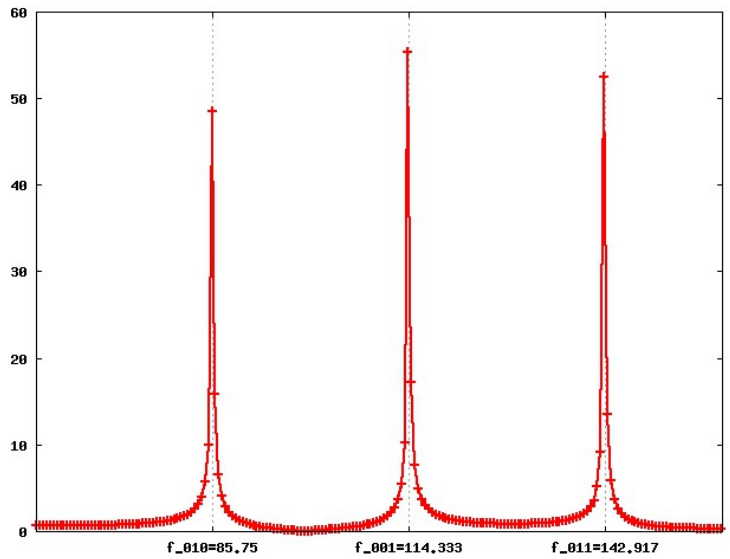

Figure 6.1: Frequency response at the monitoring mic. in the range $50 \leq f \leq 150$ Hz.

$$f_{ijk} = \frac{c_0}{2}\sqrt{\left(\frac{i}{L_x}\right)^2 + \left(\frac{j}{L_y}\right)^2 + \left(\frac{k}{L_z}\right)} \tag{6.2}$$

Figures 6.1 and 6.2 show the results for $L_x = 1.0$, $L_y = 2.0$, $L_z = 1.5$ for two different frequency ranges. The analytical values of the eigenfrequencies lying in the range are shown, to verify the accuracy of the `AcouSTO` solution.[1] It is important to notice that the modal density increases significantly with frequency. At higher frequencies, the resolution required to have a discernible sequence of peaks is not affordable. The numerical identification of the fundamental modes of vibration at high frequencies is not a trivial task, which cannot be addressed effectively with BEM or FEM. Figure 6.3 shows the fundamental modes corresponding to the eigenfrequencies identified in the frequency range

[1] An interesting exercise could be a rigorous convergence analysis of the values of the eigenfrequencies captured by `AcouSTO` as a function of the number of boundary elements.

© U. Iemma & V. Marchese

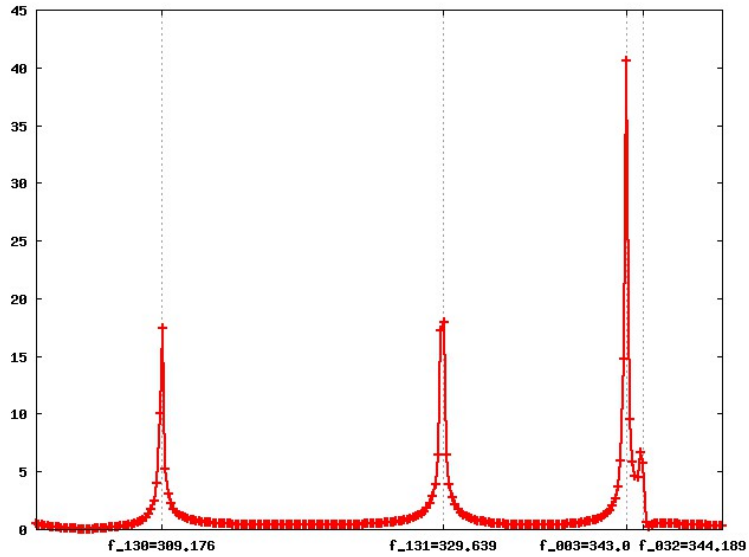

Figure 6.2: Frequency response at the monitoring mic. in the range $300 \leq f \leq 350$ Hz.

analysed. The real part of the total field is depicted on the room's walls. The user can compare the solution by activating the simple text output (`printout=1;`) and plotting the data against the solution in Eq. 6.2.

6.3 Analysis with one sound–absorbing wall

6.3.1 Source strength definition

In `AcouSTO` , the incident field generated at $\mathbf{x}$ by a generic point source located in $\mathbf{x}_s$ is calculated as

$$\tilde{\varphi}(\mathbf{x}, \omega) = \tilde{A}\, \frac{e^{-j\omega\, |\mathbf{x}-\mathbf{x}_s|/c_0}}{4\,\pi\, |\mathbf{x} - \mathbf{x}_s|} \tag{6.3}$$

where c_0 is the reference speed of sound. The complex amplitude $\tilde{A}$ is the quantity given in input in the source file pointed by the config file, and formatted according to the `AcouSTO` input convention. It is worth spending few word about this point.

The acoustic field generated by a point source can be represented both inn terms of pressure p or acoustic velocity potential ϕ. So, the physical meaning of the source itself depends on the interpretation of the unknown function $\tilde{\varphi}$. If the function $\tilde{\varphi}$ represents the acoustic pressure $\tilde{p}$, then the primary field due to the point source in $\mathbf{x}_s$ is

$$\tilde{p}(\mathbf{x}, \omega) = \tilde{S}\, \frac{e^{-j\omega\, |\mathbf{x}-\mathbf{x}_s|/c_0}}{4\,\pi\, |\mathbf{x} - \mathbf{x}_s|} \tag{6.4}$$

© U. Iemma & V. Marchese

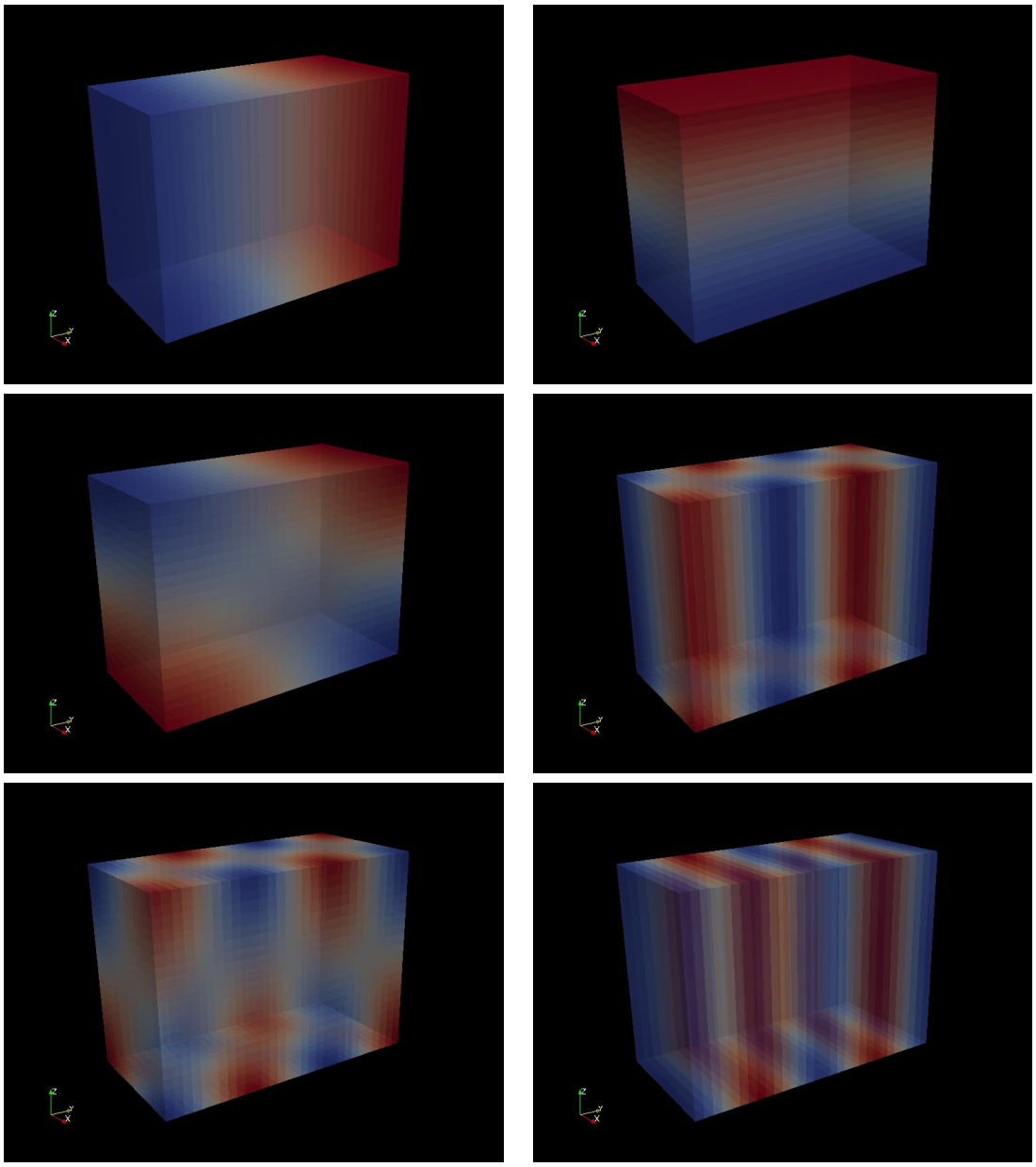

Figure 6.3: Fundamental modes Ψ_{010}, Ψ_{001}, Ψ_{011}, Ψ_{130}, Ψ_{131}, Ψ_{003}. Room size $L_x = 1.0$, $L_y = 2.0$, $L_z = 1.5$.

and its physical meaning of 6.3 is that of a source of momentum. On the other hand, if the function $\tilde{\varphi}$ represents the acoustic velocity potential ϕ, the physical meaning is that of a source of mass and the expression of the primary field can be written as

$$\tilde{\phi}(\mathbf{x}, \omega) = -\tilde{Q}\, \frac{e^{-j\omega\, |\mathbf{x}-\mathbf{x}_s|/c_0}}{4\,\pi\, |\mathbf{x} - \mathbf{x}_s|} \tag{6.5}$$

© U. Iemma & V. Marchese

where

$$\tilde{Q} = -\frac{4\,\pi \tilde{S}}{j\,\omega\,\varrho} \tag{6.6}$$

Now, the fields induced by Eqs. 6.4 and 6.11 are solutions of the non–homogeneous Helmholtz equation

$$\nabla^2 \tilde{p} + \kappa^2 \tilde{p} = 4\pi \tilde{S} \delta(\mathbf{x} - \mathbf{x}_s) \tag{6.7}$$

As a consequence, the value of the complex amplitude $\tilde{A}$ to be given as input in `AcouSTO` is related to the physical point source strength as follows:

$$\tilde{A} = 4\pi\,\tilde{S} \qquad \text{if} \quad \tilde{\varphi} \equiv \tilde{p} \tag{6.8}$$

$$\tilde{A} = \tilde{Q} = -\frac{4\pi\,\tilde{S}}{j\omega\varrho} \qquad \text{if} \quad \tilde{\varphi} \equiv \tilde{\phi} \tag{6.9}$$

Having said this, in real applications the source magnitude is often given in terms of time–averaged power output, which can be written as

$$\overline{\mathcal{P}} = \frac{2\,\pi |\tilde{S}|^2}{c_0\,\varrho} \tag{6.10}$$

Obviously, if the signal produced by the source is not monochromatic, then the contribution of each frequency band must be taken into account. Nevertheless, the small amplitude of the acoustic perturbations, and the fact that the time average of the product of harmonic functions at two different frequencies is zero, allow us to write for N_b frequency bands (see *e.g.*, [1])

$$\overline{\mathcal{P}} = \sum_{k=1}^{N_b} \overline{\mathcal{P}}_k \tag{6.11}$$

6.3.2 Wall impedance

The physical properties of a boundary can be specified in `AcouSTO` through appropriate conditions assuming that, at the boundary (or a portion of it), the unknown function and its normal derivative satisfy the equation

$$\gamma(\mathbf{x},\kappa)\,\tilde{\varphi}(\mathbf{x},\kappa) + \lambda(\mathbf{x},\kappa)\,\frac{\partial \tilde{\varphi}(\mathbf{x},\kappa)}{\partial n} = \tilde{f}(\mathbf{x},\kappa) + \tilde{\mathbf{g}}(\kappa)\cdot\mathbf{n}(\mathbf{x}), \qquad \text{for } \mathbf{x} \in \partial\mathcal{V} \tag{6.12}$$

where the complex coefficients λ, γ, the scalar function $\tilde{f}$, and the vector $\mathbf{g}$ have a physical meaning depending on $\tilde{\varphi}$. Equation 6.12 represents a so–called *locally reacting surface.*

Most likely, the properties of a generic sound–absorbing material are given in terms of the real *absorbing coefficient* α. It is thus necessary to derive an appropriate value of the complex quantities in 6.12.

For a single–frequency perturbation normally imping on the absorbing wall () having the form

$$p_I(t) = Re(\tilde{p}_I\,e^{j\omega t}) \tag{6.13}$$

© U. Iemma & V. Marchese

the reflected wave compatible with the *locally reacting surface* assumption is

$$p_R(t) = Re\left(\mathcal{R}(\omega)\,\tilde{p}_I\,e^{j\omega t}\right) \tag{6.14}$$

where $\mathcal{R}(\omega)$ is the *pressure–amplitude complex reflection coefficient*. It is related to the local impedance of the wall, $\mathcal{Z}$, by the relationship

$$\mathcal{Z}(\omega) = \varrho c_0\,\frac{1+\mathcal{R}(\omega)}{1-\mathcal{R}(\omega)} \tag{6.15}$$

whose real part is related to the absorption coefficient by

$$Re(\mathcal{Z}(\omega)) = \varrho c_0\left(1-|\mathcal{R}(\omega)|^2\right) = \varrho c_0\,\alpha(\omega) \tag{6.16}$$

It is important to notice that from the knowledge of the real number α it is possible to derive only the real part of $\mathcal{Z}$ (the *resistive* part). If the imaginary part is important to the analysis (the *reactive* part), then it must be known explicitly. Nevertheless, the reactive part represents the pressure which is in phase opposition with the particle motion, and thus is not relevant in this specific application, since it does not produce work and does not dissipate energy.

Once that $\mathcal{Z}$ is known, the coefficients in Eq. 6.12 can be derived. Recalling that from the linearized Bernoulli theorem follows that $\tilde{p} = -j\,\omega\varrho\,\tilde{\phi}$, independently on the physical meaning of $\tilde{\varphi}$, we obtain

$$\lambda = 1 + j\,0 \tag{6.17}$$

$$\gamma = 0 - j\,\frac{\omega\varrho}{\mathcal{Z}} \tag{6.18}$$

6.3.3 Application

One of the walls of the room analysed in Section 6.2 is now covered with a sound–absorbing material with $\alpha = 0.25$ (many types of wood have a similar coefficients in a wide frequency range). A monopole source is placed in the same location as in the previous analysis, but now it is amplified so as to have an average power output $\overline{\mathcal{P}} = 1$ W. If the source excites the filed at 325 Hz, according to Sections 6.3.1 and 6.3.2, it follows

Impedance $\mathcal{Z}$ (Rayls)	$103.76 + j\,0.0$
λ	$1 + j\,0$
γ	$0 - j\,23.813$
Source amplitude $\tilde{S}$	102.16 + j 0.0

The analysis can be performed either by providing an impedance file using the directive `imped_file="filename"`, or by providing the values of λ and γ, setting `custombc =1`

© U. Iemma & V. Marchese

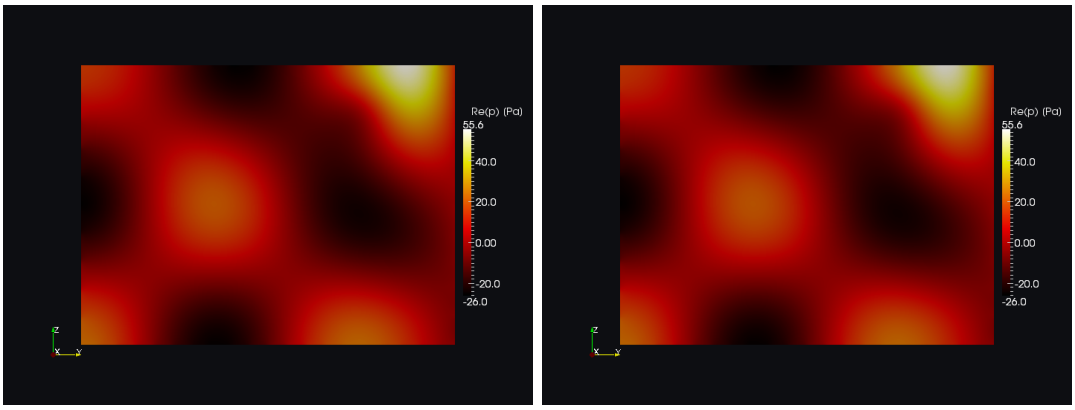

Figure 6.4: Acoustic field calculated on one layer of microphones, in presence of absorbing material on the xz–wall at $y > 0$. Directive `imped_file` was used on the left, whereas the `custombc` approach on the right.

in the configuration files. Both options are provided with the tutorial. The solution is presented in Fig. 6.4 for the two approaches. The fields obtained are absolutely identical. The user could verify the accuracy of the solution by comparing it with the results of other simulation tools. Figure 6.5 shows the qualitative comparison of the SPL obtained with `AcouSTO` with that obtained with a commercial FEM software. The agreement is qualitatively very good, even if some difference could be noticed, primarily due to the not identical color scale used, and to the higher resolution of the `AcouSTO` layer of microphones.

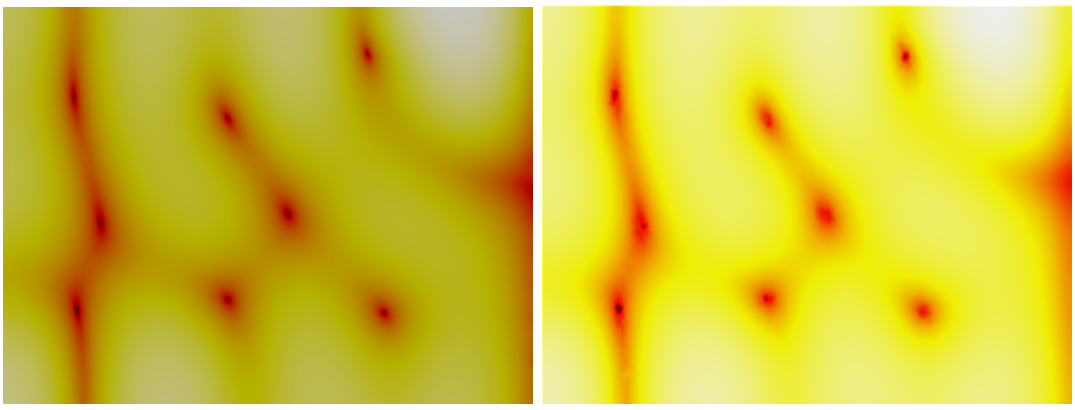

Figure 6.5: Comparison of `AcouSTO` results (left) with FEM analysis using a commercial software.

© U. Iemma & V. Marchese

CHAPTER 7

Incompressible Potential Aerodynamics

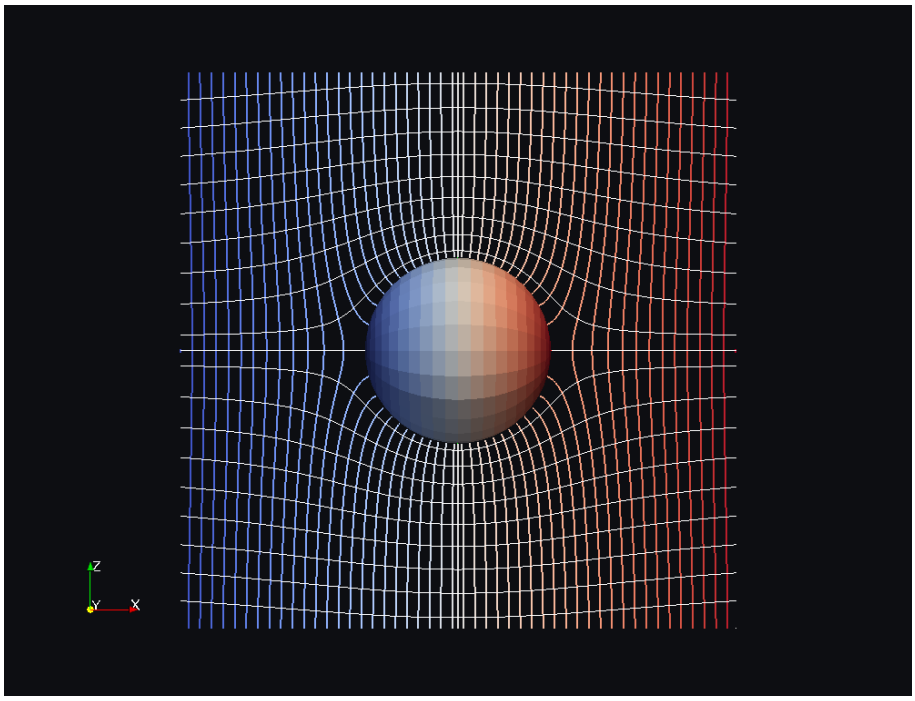

Steady flow around blunt bodies
(... This is tricky. Handle with care ...)

In this last tutorial, we take advantage of the flexibility of the custom boundary conditions to use `AcouSTO` for the solution of the limit form of the Kirchhoff-Helmholtz BIE for $\omega \to 0$. What we are going to obtain is the solution of the Laplace equation for the specific case of an incompressible potential flow, but the same approach can be applied, in principle, to any stationary physical problem governed by the Laplace or Poisson equations. The user must be aware of the fact that this use of the code is somehow "borderline" and one must not expect to be able to solve any kind of potential problem. For instance, the presence of surfaces of discontinuity for the function $\tilde{\varphi}$ cannot be treated, and thus the analysis of lifting bodies (wings or propeller blades) is not possible.

7.1 Potential flow of an incompressible, inviscid fluid

Consider the flow of an inviscid, incompressible fluid such that, at a certain instant in time, the velocity field $\mathbf{v}$ is *irrotational*, *i.e.*, $\nabla \times \mathbf{v} = 0$ everywhere. Under this hypothesis, and assuming that no source of vorticity are present in the field, Kelvin's theorem ensures that the flow remains irrotational at all times, and thus it exists the *aerodynamic velocity potential* ϕ such that $\mathbf{v} = \nabla\phi$. The continuity equation for such a flow is $\nabla \cdot \mathbf{v} = 0$, which, in terms of ϕ, reduces to the Laplace equation

$$\nabla^2\phi = 0, \qquad \mathbf{x} \in \mathcal{V} \tag{7.1}$$

where $\mathcal{V}$ indicates the domain occupied by the flow. It can be easily demonstrated that such a problem can be recast in the integral form

$$E(\mathbf{y})\phi(\mathbf{y}) = \oiint_{\partial\mathcal{V}} \left(G_0 \frac{\partial\phi}{\partial n} - \phi \frac{\partial G_0}{\partial n} \right) \mathrm{d}\mathcal{S} \tag{7.2}$$

where the domain function $E = 1, 0.5, 0$ if $\mathbf{y} \in \mathcal{V}$, $\mathbf{y} \in \partial\mathcal{V}$ or $\mathbf{y} \notin \mathcal{V}$, respectively, and where

$$G_0(\mathbf{x}, \mathbf{y}) = \frac{-1}{4\pi\ |\mathbf{x} - \mathbf{y}|} \tag{7.3}$$

is the solution of

$$\nabla^2 G_0 = \delta(\mathbf{x} - \mathbf{y}), \qquad \mathbf{x} \in \mathcal{V} \tag{7.4}$$

$$\text{with } \ \phi \to 0 \ \text{ for } \ \mathbf{x} \to \infty \tag{7.5}$$

i.e., the *free–space Green's function* of the Laplacian

Equations 7.1, 7.3, and 7.2 can be seen as the stationary limits of the wave equation, its fundamental solution, and the corresponding BIE formulation, respectively. Or, equivalently, the they can be obtained as the limit for the frequency tending to 0 of the Helmholtz equation, its fundamental solution, and the Kirchhoff–Helmholtz BIE.

Specifically, this second interpretation can be easily verified by taking the limit for $\omega \to 0$ of the equation presented in the theoretical introduction of the `AcouSTO` manual. In the following sections we will see how `AcouSTO` can be used to solve a problem governed by such equations.

© U. Iemma & V. Marchese

7.2 Files

The files provided with this tutorial are under

`acousto_distribution_path/tutorials/Potential_Aerodynamics`

and are listed below.

Name	Content
`potaero.cfg`	Configuration file
`g.file`	custom boundary conditions **g** file
`mics.geo`	`Gmsh` file for the layer of microphones

7.3 Impermeable sphere in a uniform flow

Consider an impermeable sphere of radius a immersed within an inviscid flow whit undisturbed velocity $\mathbf{V}_0$. The presence of the sphere induces a perturbation of velocity field, and local velocity $\mathbf{u}$ can be seen as the superposition of the undisturbed velocity, and the perturbation $\mathbf{v}$ induced by presence of the body, $\mathbf{u}(\mathbf{x}) = \mathbf{V}_0 + \mathbf{v}(\mathbf{x})$. The velocity potential of such a flow can be obtained analytically by superposition of the potential of a uniform stream and that of a mass point source located in the center of the sphere. Assuming the undisturbed stream aligned with the x–axis, the exact solution is given by

$$\Phi = V_0\, x \left[1 + \frac{a^3}{2\left(x^2 + y^2 + z^2\right)^{3/2}} \right] \tag{7.6}$$

where $\Phi_0 = V_0\, x$ is the potential of the undisturbed stream, whereas the remaining part is the perturbation potential ϕ such that $\nabla\phi = \mathbf{v}$.

7.3.1 How to solve the problem with `AcouSTO`

The solution of the problem with `AcouSTO` can be addressed through an appropriate definition of the boundary conditions. The impermeability of the body implies that the velocity of the fluid particles in contact with the sphere boundary cannot have a normal component different from zero. Thus, indicating with $\mathbf{n}$ the unit normal to the sphere surface pointing into the fluid, impermeability implies that

$$\mathbf{u}\cdot\mathbf{n} = 0 \quad \Rightarrow \quad \mathbf{v}\cdot\mathbf{n} = \nabla\phi\cdot\mathbf{n} = -\mathbf{V}_0\cdot\mathbf{n} \quad \Rightarrow \quad \frac{\partial\phi}{\partial n} = -\mathbf{V}_0\cdot\mathbf{n} \tag{7.7}$$

Recalling Eq. 6.12, it follows that the conditions 7.7 can be applied by setting

$$\lambda = 1, \;\; \gamma = 0, \;\; \tilde{f} = 0, \;\; \tilde{\mathbf{g}} \equiv -\mathbf{V}_0 \tag{7.8}$$

© U. Iemma & V. Marchese

Obviously, the angular frequency must be set to 0 in the configuration file. The result obtained with $V_0 = 1\ m/s$ is presented in Figure 7.1. Specifically, the density plot of the perturbation potential around the sphere is depicted, with the streamlines of the flow superimposed as black continuous curves. Figure 7.2 shows the comparison of the numerical results with the exact solution of Eq. 7.6 along two straight lines, revealing a remarkable agreement in both cases.

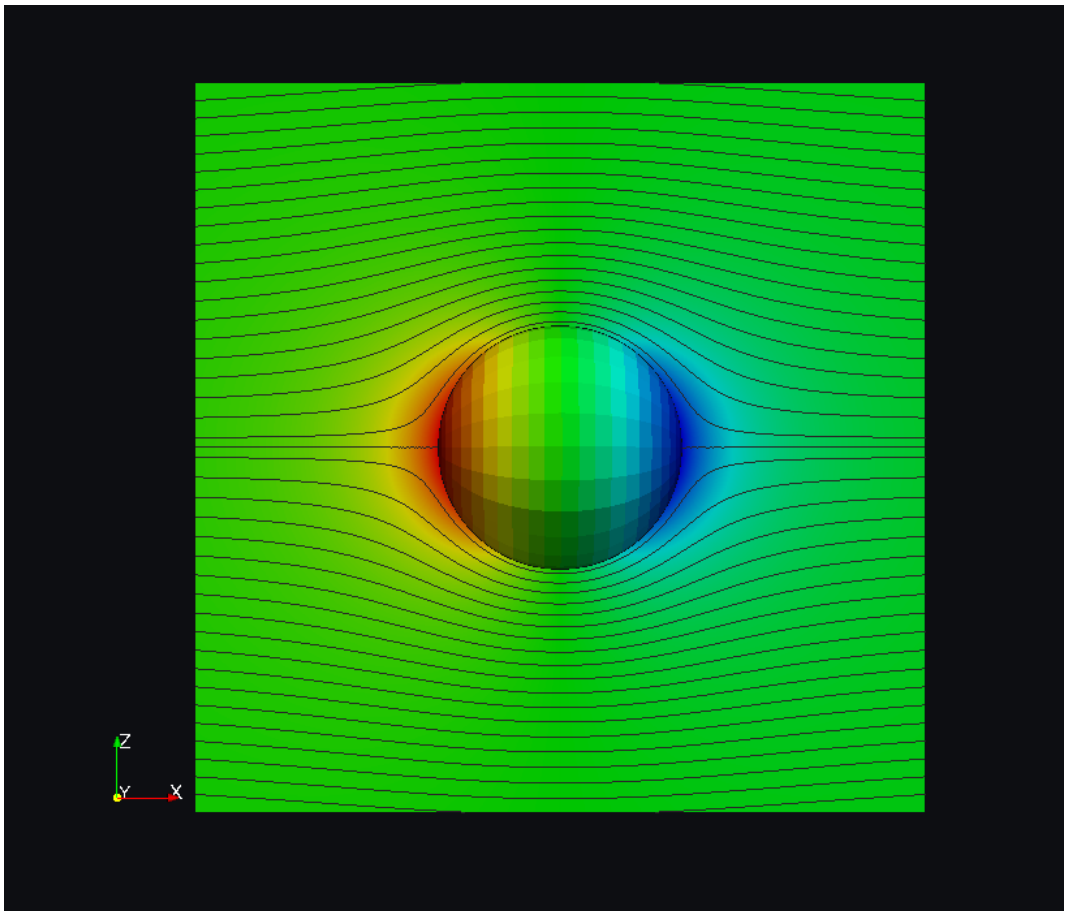

Figure 7.1: Perturbation velocity potential distribution around a sphere within a main stream with undisturbed velocity $\mathbf{V}_0$ aligned with the x–axis. Streamlines are represented by black continuous lines.

© U. Iemma & V. Marchese

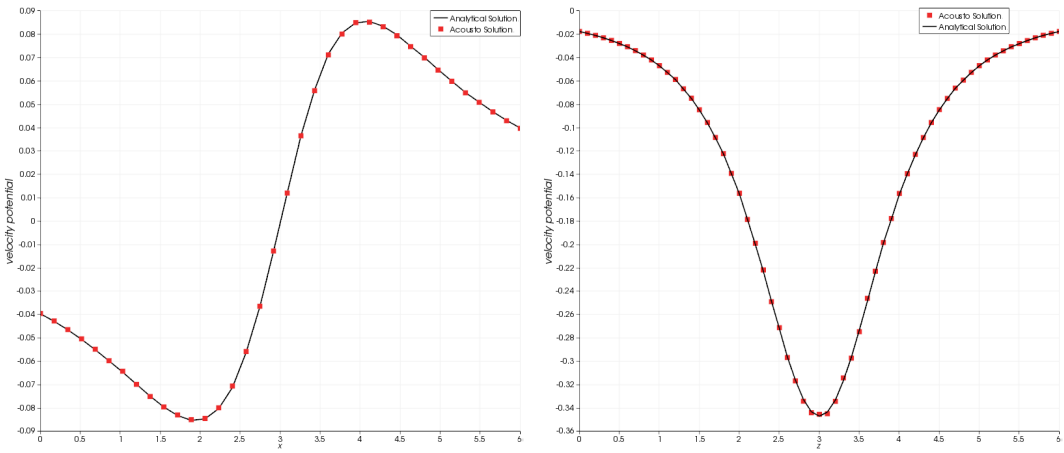

Figure 7.2: Comparison of `AcouSTO` results with the analytical solution along two sections of the domain at constant z (left) and constant x (right).

© U. Iemma & V. Marchese

Bibliography

[1] A. D. Pierce, Acoustics - An Introduction. Its Physical Principles and Applications, Acoustical Society of America, New York, 1989.

[2] Crighton, D.G., Dowling , A.P., Ffowcs Williams, J.E., Heckl, M., Leppington, F.G., Modern Methods in Analytical Acoustics - Lecture Notes, Springer-Verlag, London, 1992.

[3] Morse, P.M.C. and Ingard, K.U., Theoretical Acoustics, International series in pure and applied physics, Princeton University Press, Princeton, 1968.

[4] Umberto Iemma and Vincenzo Marchese, `AcouSTO` User Manual v1.6, http://acousto.sourceforge.net, 2013.

[5] David L. Colton and Rainer Kress, Integral equations methods in scattering theory, *Pure and Applied Mathematics Series*, Krieger Publishing Company, 1992.